X-644-71-360
PREPRINT

NASA TM X-65695

TERRESTRIAL AND LUNAR ANALOGUES OF MARTIAN TOPOGRAPHY

PAUL D. LOWMAN, JR.

SEPTEMBER 1971

GSFC
GODDARD SPACE FLIGHT CENTER
GREENBELT, MARYLAND

X-644-71-360

TERRESTRIAL AND LUNAR ANALOGUES OF MARTIAN TOPOGRAPHY

Paul D. Lowman, Jr.

September 1971

GODDARD SPACE FLIGHT CENTER
Greenbelt, Maryland

TERRESTRIAL AND LUNAR ANALOGUES OF MARTIAN TOPOGRAPHY

Paul D. Lowman, Jr.

ABSTRACT

A comparison has been made among Mariner 6 and 7 photographs of Mars and orbital photographs of the earth and moon to see if any Martian terrain features were similar to terrestrial or lunar features of comparable size. Five general categories of similarity were found. Tectonic basins were inferred to exist on Mars from the similarity of the border scarps of the Hellas basin to fault scarps of the Brokeoff Mountains in New Mexico. Hellas was interpreted as a tectonic basin filled with wind-deposited sand, as is the Marzuk basin of North Africa. It is structurally analogous to the basin occupied by the Gulf of Mexico. Crustal collapse structures were inferred from the general similarity of the martian chaotic terrain to the physiography of the eastern Mojave Desert and the Afar depression. The chaotic terrain was interpreted as a form of tectonic collapse analogous to ocean floor spreading and its continental extension. Eolian deposits of sand on Mars were suggested by the similarity of light areas previously mapped as chaotic terrain to linear ergs in the western Sahara; however, there should be gradations between chaotic terrain and sand-filled depressions. Light areas in craters of Meridiani Sinus, if interpreted as lee dunes, suggest the same general wind direction (NE to SW) as the supposed linear ergs. Mare ridges essentially identical to those of lunar maria were found in one Mariner photograph, suggesting that the martian crust may be volcanic despite

the apparent absence of moon-like maria. A sinuous rille system over 200 kilometers long was found on one Mariner photograph; the absence of evidence for fluvial erosion suggest that both martian and lunar sinuous rilles are of internal origin. Martian tectonic activity is inferred to be mild by terrestrial standards, and to involve chiefly vertical movement. The chaotic terrain may represent incipient crustal fragmentation; if so, it would suggest by analogy that terrestrial crustal evolution has been a process of continental fragmentation and thickening by ocean-floor spreading and underthrusting, rather than of continental growth.

CONTENTS

INTRODUCTION

The high resolution of the Mariner 6 and 7 photographs of Mars permits much more specific comparisons of Martian physiography with that of other planets than has previously been possible. This paper presents results of such a comparison, using orbital photographs of the earth and moon, whose objective was to find out if the physiographic features of Mars could be matched with those of the earth or the moon.

Comparisons between Mars and the earth have been frequently made, but since the Mariner 4 revelation of the abundant Martian craters, Mars has generally been compared to the moon. The stress in this paper will be on similarities between the earth and Mars, using orbital photographs of comparable scale and resolution.

The pictures used in this study were, first, those transmitted by the Mariner 6 and 7 spacecraft. These have been described by Leighton, et al. (1969). Lunar photographs used were from Lunar Orbiter spacecraft (Kosofsky and El Baz, 1970) and various Apollo lunar missions. Orbital photographs of the earth were taken during Gemini and Apollo earth orbital missions, generally as part of the Synoptic Terrain Photography Experiment (Lowman and Tiedemann, 1971). One Nimbus I Advanced Vidicon Camera System picture was used; this system is described in the "Nimbus I Users' Catalog: AVCS and APT," Goddard Space Flight Center, 1965.

It has been found that similarities between terrain features of Mars and those of the earth and moon fall into five general categories. These categories are neither equivalent nor entirely objective; they are primarily a convenient means of organizing the material.

Index maps and photographs of Mars and North Africa are presented in Figures 29 and 30.

TECTONIC BASINS

The first Martian terrain feature to be discussed is Hellas, a roughly circular light area about 1700 km in diameter in the southern Hemisphere, bounded on the west by the linear dark area Hellespontus (Fig. 1). When examined more closely through selected Mariner photographs (Figs. 2, 3, and 4), Hellas is seen to be featureless at this resolution (Sharp, et al., 1971a) and Hellespontus cratered. Hellas has been inferred to be a topographic basin from the photographic, radio, and CO_2 pressure data from Mariner 7.

The features of greatest interest in this series of photographs are the linear ridges on the slope between Hellespontus and Hellas. As Sharp and his colleagues point out, these are probably scarps related to the formation of Hellas. The isolated ridges are on the order of 20 to 40 kilometers long in this region, although they probably grade into longer one-sided scarps elsewhere. These ridges appear to have terrestrial counterparts in the Brokeoff Mountains of southern New Mexico, which were photographed from Apollo 6 (Fig. 5). The Brokeoff Mountains are a series of fault scarps and blocks along which the Salt Basin has

been down-faulted relative to the Guadalupe Mountains and the Delaware Mountains of Texas. The individual ridges in the Brokeoff Mountains are somewhat shorter than those of the Hellespontus-Hellas slope, being typically 5 to 10 kilometers long. However, the entire series of faults is at least 80 kilometers long, even excluding those of the Sacramento Mountains, which are in turn part of the much longer Rio Grande rift system (Eardley, 1962). It seems safe to say that the scarps in the Hellespontus-Hellas region are of the same order of size as those of the Brokeoff Mountains. There is no first-order size discrepancy such as that encountered frequently in comparisons of terrestrial and lunar structures.

Whether the Hellas basin as a whole has any terrestrial analogues is not clear. The most visually similar feature shown on earth orbital photographs is the Marzuk basin of southern Libya (Fig. 6). This is a roughly circular depression about 370 km wide occupied by the Marzuk sand sea. Structurally, it is not quite analogous to the Hellas basin, in being bordered by cuestas rather than concentric faults. Furthermore, it is only about one-fifth the diameter of Hellas. Comparable size discrepancies also argue against other possible terrestrial examples, such as the Michigan basin (about 500 km diameter).

The most similar terrestrial structure would perhaps not be recognized as such from its topography alone: the basin occupied by the Gulf of Mexico and adjacent coastal plain. Measured from structural boundaries, this basin is about the same size as Hellas, roughly 1800 km wide E-W and N-S. It is bounded on the north, west, and south by normal faults (inward side down) and inward-dipping

sediments, although its structure on the southeast is complicated by Cuba and the Bartlett fault zone. The nature and origin of the Gulf of Mexico basin are not understood (see, for example, the discussion by Spencer, 1969, p. 336 ff), so the possible analogy between it and the Hellas basin will not be pursued further at this time.

Turning again to Mars, we see another group of structures with at least a superficial resemblance to the border scarps and fault blocks around Hellas. These are a series of light-toned linear features (Figs. 7 and 8), with apparent lengths on the order of 100 to 200 km, bordering the Central Polar Region near the south pole (Sharp, et al., 1971b). The Mariner investigators found these features "truely enigmatic." It is not even clear, for example, whether they are positive or negative topographically, although Sharp and his colleagues thought they might be scarps. Other suggested possibilities were moraines, ice ridges, or longitudinal dunes.

When viewed in regional context, and in comparison with the Hellas basin, the scarp interpretation seems most reasonable. The south polar features are concentrically arranged, and parallel to what looks like a scarp separating cratered from uncratered terrain (Fig. 8 lower right). The relations are thus the same as those of the Hellas scarps. It is not clear whether the south polar region is a basin, but a down-faulted basin filled with ice should have this general appearance. It is therefore suggested that this area is a tectonic basin similar in structure to the Hellas basin.

Before going on to the next category of terrestrial analogues, some justfication must be given for the identification of Hellas as tectonic rather than impact or volcanic (possibilities discussed by Sharp, et al. (1971a)). A volcanic origin will be dismissed, somewhat arbitrarily, because there is no terrestrial volcanic depression or composite depression even approaching this size, as Sharp, et al., point out. The impact theory requires more discussion. Hellas has a superficial resemblance to the Imbrium basin (Fig. 9), which is 1100 km wide. The Imbrium basin and other circular mare basins are widely considered to be large impact craters, now filled with ultrabasic volcanics. A full discussion of the volcanic-impact controversy is not possible here (for general discussion, see Lowman, 1970). Because of the weight of evidence, including the fragmental nature of the Fra Mauro samples returned by the Apollo 14 astronauts, it will be assumed that the Imbrium basin is primarily of impact origin.

The main evidence against an impact origin for the Hellas basin is the absence of any radial topographic features resembling the so-called Imbrium sculpture (Fig. 10), which is clearly related to the origin of the Imbrium basin (probably as horst-and-graben structures produced by the impact). Furthermore, as pointed out by Sharp, et al., there is no trace of an ejecta blanket corresponding to the Fra Mauro formation, either as hummocky topography or as an obvious deficiency in craters around Hellas. Some form of tectonic origin for the Hellas basin thus seems indicated by elimination, in addition to the positive evidence previously presented.

CRUSTAL COLLAPSE STRUCTURES

The most mysterious terrain features photographed by the Mariner 6 and 7 spacecraft were the rough, depressed uncratered areas labeled "chaotic terrain" by the Mariner investigators (Figs. 11, 12, and 13). Possible terrestrial and lunar counterparts of the chaotic terrain discussed and rejected by Sharp, et al. (1971a) include impact ejecta, volcanic collapse structures, and complex sand dunes. Because the chaotic terrain clearly seems to have formed at the expense of the surrounding cratered terrain, it was considered by Sharp and his colleagues to be some sort of mass movement. They suggested that it might be essentially internal in origin, perhaps indicating the beginning of Martian geothermal evolution.

Part of the difficulty in finding terrestrial examples of choatic terrain is its scale. The embayment shown in Fig. 13, for example, is about 50 km wide at the bottom of the picture, and is only part of a much larger area of chaotic terrain (Fig. 12). Furthermore, individual elements (hills or blocks?) are several kilometers in size. No form of mass-wasting known on the earth or moon affects such large areas.

The scale of the chaotic terrain makes it an especially good subject for comparison by study of terrestrial orbital photographs, which typically cover areas measuring 100 to 300 km on a side. Several potential terrestrial analogues have been found. One of these, the Marzuk basin, has already been presented. Its relation to chaotic terrain rests on the similarity of the fault blocks previously

discussed to the linear features bordering the long area of chaotic terrain shown in Figure 12. The resolution of this A-camera picture is not enough to permit firm identification of these features, but to the south (Fig. 12) they grade into what are clearly fissures or scarps along which the higher terrain is being converted to chaotic terrain. The chaotic terrain here is thus at least bounded, like the Hellas basin, by faults, and its continuity with them suggests that it may be a complex array of fault blocks.

A more suggestive terrestrial counterpart to the chaotic terrain was photographed by the Apollo 9 crew (Fig. 14). This is the Afar depression, an extremely interesting part of the African rift valley system that is believed by Mohr (1970) and others to represent incipient continental fragmentation. Most of the landscape shown in Figure 16 is the direct result of faulting and vulcanism; the linear ridges are fault scarps and the valleys down-faulted blocks filled with alluvium and evaporites. The picture covers roughly the same area as does the Mariner picture (Fig. 13), so the structural units are the same general size as at least the border faults of the chaotic terrain. They are, however, much more regular than the chaotic terrain despite the presence of numerous cross faults in the Afar Triangle.

A fundamentally tectonic terrain that comes closer to matching the irregularity of the chaotic terrain (Fig. 15) is shown in Figure 16. This Nimbus I television picture covers an area of southern California measuring about 320 km on a side with ground resolution on the order of half a kilometer (the Mariner picture

of Fig. 15 is 108 by 158 km). The west part of the area is dominated by the great northwest-trending wrench faults of the San Andreas family. The eastern part - the Mojave desert - is a much more irregular mosaic of fault blocks separated by light-toned alluvium-filled valleys (Fig. 17). If allowance is made for the effects of subaerial erosion and deposition in the terrestrial photographs, it seems clear that the eastern part of the Mojave block is fundamentally similar to the chaotic terrain in scale and geometry.

Assuming the resemblances just proposed to have some validity, the question arises as to what they imply for the origin of the chaotic terrain. In answer, it must first be pointed out that the Marzuk basin is fundamentally different in origin from the structures of Afar depression and the Mojave desert in being the result of cratonic basin-and-swell deformation (Lowman, 1968). The Afar depression and the Basin-and-Range province, by contrast, are areas in which oceanic ridge systems (with median rifts) intersect continental crust. In terms of modern tectonics, they are zones in which a process like sea-floor spreading is taking place under continents, leading to crustal collapse and perhaps ultimately to continental fragmentation. This process, reduced to essentials, is similar to that proposed by Sharp and his colleagues for the formation of martian chaotic terrain. On earth, ocean-floor spreading, if it occurs at all (a point not universally conceded), has been going on for much of the earth's history. Its martian counterpart has either just begun or, if the Martian cratered terrain is indeed primordial, perhaps never progressed very far.

EOLIAN DEPOSITS

Mars has traditionally been compared to terrestrial deserts (e.g., Weaver, 1970). The most recent such comparison has been made by Lowman and Tiedemann (1971) who suggested, on the basis of orbital photographs of North Africa and other deserts, that the dark areas on Mars are relatively high bedrock plateaus and the light areas lower regions filled with light-colored alluvium or wind-blown sand. (Their study was made before the availability of Mariner 6 and 7 photos.) As Cutts, et al., (1971) point out, there is so far no such consistent correlation between terrain elevation and albedo. However, a number of areas are visible on the Mariner 6 and 7 photographs that can be interpreted as deposits of wind-blown sand.

The first of these (Figs. 18 and 19) is centered on Long. 320°W, Lat. 15°S, and includes a series of linear bright features with a regional braided pattern. A similar group of bright features is shown in Figure 11 near Long. 45°W on the Martian equator and, in more detail, in Figure 20. Both have a north to northeast trend, and are at least several hundred kilometers long and several score kilometers wide. The second of these areas has been interpreted by Sharp, et al. (1971a) as chaotic terrain because it seems to be continuous with the area of chaotic terrain previously discussed (Fig. 12).

Gemini and Apollo photographs of northeast Africa reveal several linear ergs with a striking resemblance to the Martian features. These are sand dune areas parallel to the prevailing northeast winds, measuring up to some 500 km in length

and perhaps 50 km in width. It is difficult to put an upper limit on the dimensions of these features, since some of them (e.g., the erg in Fig. 6 north of the Marzuk sand sea) grade into large non-linear dune fields. An important point brought out by these photographs is that the ergs have remarkable sharp boundaries. This may solve a problem discussed for Mars by Cutts, et al., who felt that the sharp boundaries of the Martian features argued against dust deposition. The Saharan ergs are probably composed of sand-sized particles, transported by traction and saltation as suggested by Cutts and colleagues for Mars. It must be remembered that the Martian atmosphere is far thinner than that of earth, so analogies of this sort must be suggested cautiously.

Returning to Figure 18 and a close-up of the central section (Fig. 24), we see another class of possible eolian deposits, in Meridiani Sinus. It was suggested by Cutts, et al., that the light-toned material preferentially located in the north floors of many craters might be wind-deposited, subject to the problem of sharp boundaries just discussed. There is little to add here to their treatment, but if these light areas are in fact dunes deposited in the lee of crater walls, it would suggest a general north to south wind direction. Referring to Figure 18, we see that this would be consistent with the interpretation of the light-toned linear features farther west as ergs parallel to the prevailing winds.

It should be added that the erg interpretation does not necessarily contradict the suggestion by Sharp, et al., that these areas are chaotic terrain. Chaotic terrain is lower than the surrounding areas, and it would be expected to fill with

wind-blown sand under the right conditions of wind direction and sand supply. If the interpretations proposed here, both of structure and geomorphology, are correct, the Mariner 71 photographs should show all gradations between chaotic terrain and featureless terrain.

LUNAR ANALOGUES

Comparisons between Mars and the moon have been almost exclusively focused on the craters common to both. However, there are at least two examples of topographic feature typical of the moon that are shown on the Mariner 6 and 7 photos.

The first of these is a ridge on the order of 60 km long in the Deucalionis Regio (Fig. 25 and mosaic Fig. 18). This ridge appears essentially similar in size and shape to lunar mare ridges such as those in Sinus Medii (Fig. 26). The origin of the lunar mare ridges is not understood. (A summary of current theories is given by Lowman, 1969.) However, they are exclusively associated with mare material, now known to be ultrabasic volcanic rock. Many workers favor the theory that the ridges are the fissures from which the eruptions came, now occupied by late differentiates of the mare magmas that have, in some areas, been extruded (O'Keefe, et al., 1967). Regardless of their actual nature, the similarity between the lunar mare ridges and the one photographed by Mariner 6 suggests that much of the Martian surface may be volcanic, despite the apparent absence of maria such as those found on the moon. In this connection, it should be pointed out that Sinus Medii is itself a highland mare, not occupying a

circular basin as do some maria; hence there may be no contradiction between the absence of maria and the presence of mare ridges on Mars.

A second topographic feature that may be common to the moon and Mars is the sinuous rille. An example of this feature (the only one so far) is shown in Figure 27, with a Lunar Orbiter photo of sinuous rilles near the lunar crater Prinz for comparison (Fig. 28). The Martian rille system is relatively inconspicuous on the A-camera photograph, but in fact is as large as any on the moon, with a length of over 200 km. The origin of lunar sinuous rilles is still controversial, although the anhydrous mineralogy of the Apollo samples has discredited the fluvial erosion theory. The finding of a familiar but poorly-understood feature on Mars would not, a priori, be expected to throw much light on Martian geology. However, the general lack of any other possible evidence for fluvial erosion on Mars, which has been apparent since Mariner 4, tends to support an internal origin for sinuous rilles in general. Further speculation is unwarranted at this time.

SUMMARY AND CONCLUSIONS

This study indicates that, contrary to preliminary opinions, the Mariner 69 photographs of Mars do reveal tectonic and topographic forms fundamentally similar to some found on earth. The tectonic activity inferred to have taken place in Mars is mild compared with terrestrial tectonism, consisting primarily of vertical regional movements accompanied by normal faulting. The best established example of this is the Hellas basin. If the structure and origin of the

chaotic terrain have been correctly deduced, it may represent an incipient stage of crustal fragmentation analogous to ocean floor spreading on earth. Should this be verified by future Mars missions, it might provide further support for the theory that crustal evolution on the earth has been chiefly a process of fragmentation and underthrusting whereby an originally global continental crust has become smaller in extent but thicker (Lowman, 1969). The fact that this theory is in direct contradiction to currently favored theories of continental growth adds to the geologic interest of Mars.

ACKNOWLEDGEMENTS

I am indebted to Dr. R. P. Sharp, California Institute of Technology, for the use of his collection of Mariner 6 and 7 photographs and supporting data during a visit in August 1971.

The Mariner prints used in this report were supplied by the National Space Science Data Center, Goddard Space Flight Center.

REFERENCES

Cutts, J. A., Soderblom, L. A.. Sharp, R. P., Smith, B. A., and Murray, B. C., 1971, The surface of Mars, 3: Light and dark markings: Jour. Geophys. Res., v. 76, no. 2, p. 343-356.

Eardley, A. J., 1962, Structural Geology of North America: Harper & Row, New York, 743 p.

Kosofsky, L. J., and El-Baz, F., 1969, The Moon as Viewed by Lunar Orbiter: NASA Special Publication 200, Government Printing Office, Washington, D.C.

Leighton, R. B., Horowitz, N. H., Murray, B. C., Sharp, R. P., Herriman, A. H., Young, A. T., Smith, B. A., Davies, M. E., and Leovy, C. B., 1969, Mariner 6 and 7 television pictures: preliminary analysis: Science, v. 166, no. 3901, p. 49-67.

Lowman, P. D., Jr., 1968, Space Panorama: WELTFLUGBILD Reinhold A. Muller, Feldmeilen/Zurich, Switzerland, 140 p.

Lowman, P. D., Jr., 1969, Geologic orbital photography: experience from the Gemini Program: Photogrammetria, v. 24, p. 77-106.

Lowman, P. D., Jr., 1970, The geologic evolution of the moon: X-644070-381, Goddard Space Flight Center, Greenbelt, Maryland.

Lowman, P. D., Jr., and Tiedemann, H. A., 1971, Terrain photography from Gemini spacecraft: final geologic report: X-644-71-15, Goddard Space Flight Center, Greenbelt, Maryland.

Mohr, P. A., 1971, Ethiopian rift and plateaus: some volcanic petrochemical differences: Jour. Geophys. Res., v. 76, no. 8, p. 1967-1984.

O'Keefe, J. A., Lowman, P. D., Jr., and Cameron, W. S., 1967, Lunar ring dikes from Lunar Orbiter I: Science, v. 155, p. 77-79.

Sharp, R. P., Soderblom, L. A., Murray, B. C., and Cutts, J. A., 1971, The surface of Mars, 2: Uncratered terrains: Jour. Geophys. Res., v. 76, no. 2, p. 331-342.

Sharp, R. P., Murray, B. C., Leighton, R. B., Soderblom, L. A., and Cutts, J. A., 1971b, The surface of Mars, 4: South polar cap: Jour. Geophys. Res., v. 76, no. 2, p. 357-368.

Spencer, E. W., 1969, Introduction to the Structure of the Earth: McGraw-Hill Book Co., New York, 597 p.

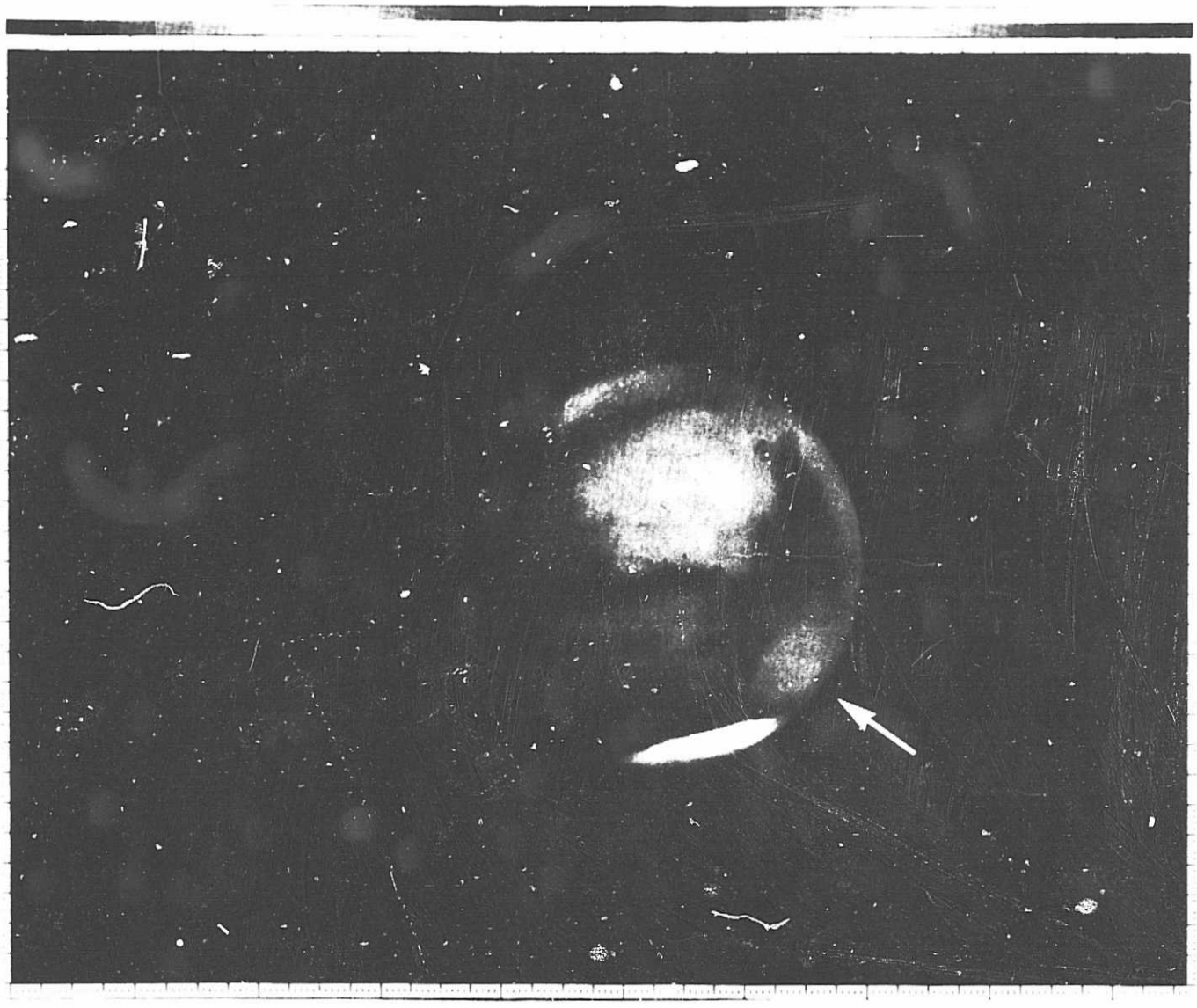

Figure 1. Mariner frame 7F67, B camera (508 mm focal length), from 710,814 km range, showing Mars with north at top. Hellas indicated by arrow.

Figure 2. Mariner frame 6F49, B camera, from 206,681 km range, showing Hellas at lower right.

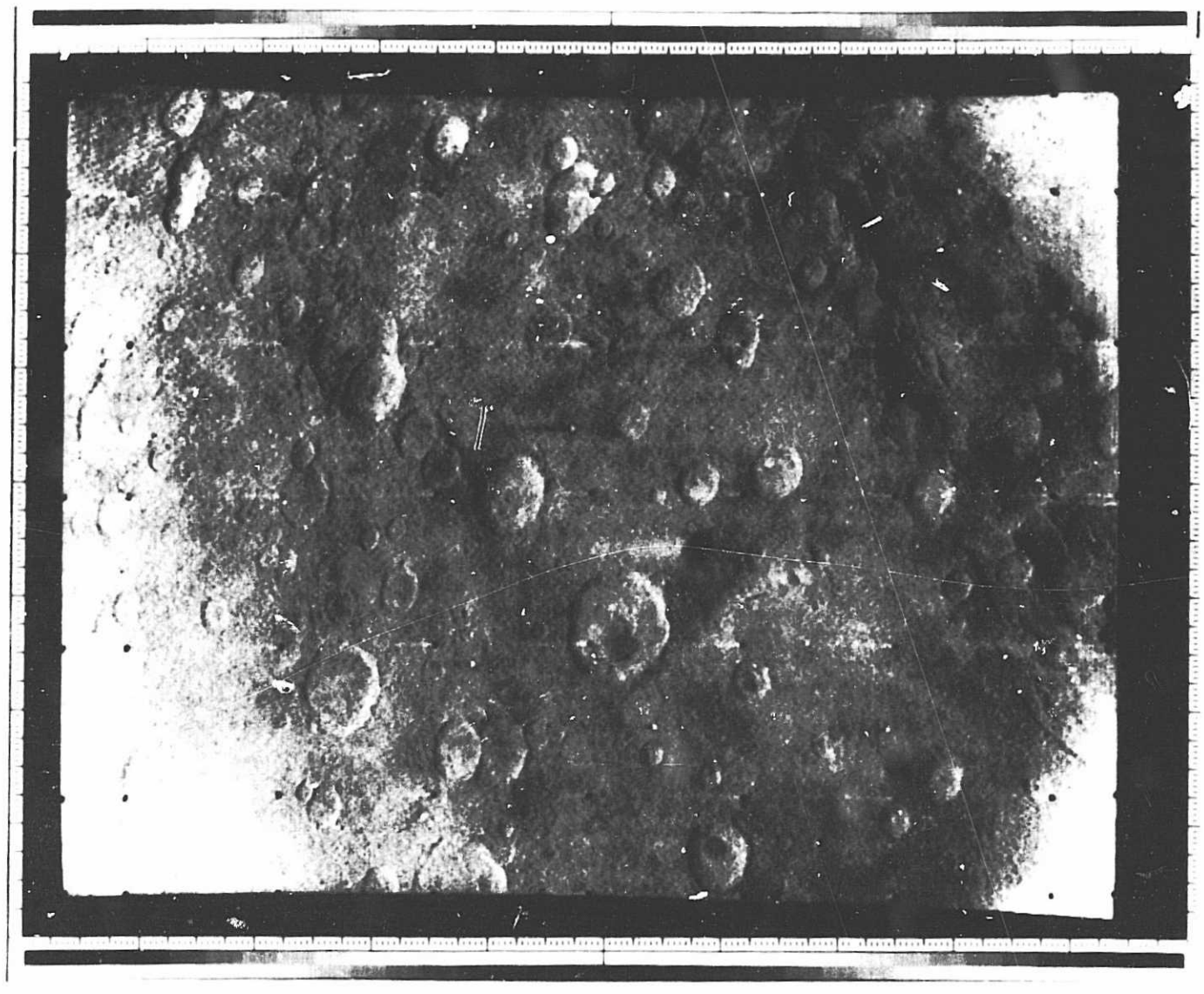

Figure 3. Mariner frame 7N25, A camera (52.5 mm focal length), showing cratered terrain of Hellespontus. North at top; area covered 1228 by 723 km. Slope down into Hellas basin at upper right. This and all other photos are "Maximum discriminability" versions unless otherwise labeled.

Figure 4. Mariner frame 7N27, A camera, showing slope from Hellespontus into Hellas. Area covered 998 by 723 km; overlaps previous picture. Black dots are reseau marks; white streaks to their left are artifacts caused by slow decay of automatic gain control (Dunne, et al., 1971).

Figure 5. Apollo 6 photo AS 6-2-1450, covering area averaging 150 km square in southern New Mexico and west Texas; north at bottom. Landmarks as follows: cb - Carlsbad, N.M.; P - Pecos River; C - Guadalupe Ridge (exhumed Paleozoic reef); H - Huapache monocline; B - Brokeoff Mountains; GM - Guadalupe Mountains; D - Delaware Mountains; S - Salt Basin (squares are cultivated land); Y - Y-O Structural Zone (Dane and Bachman, 1964); SM - Sacramento Mountains. Scratch-like mark above "B" is scratch. Most of area underlain by late Paleozoic carbonates. West face of Guadalupe Mountians is fault scarp, with east side (left) upthrown. Brokeoff Mountains are fault slices; compare with scarps in Figures 3 and 4 between Hellas and Hellespontus.

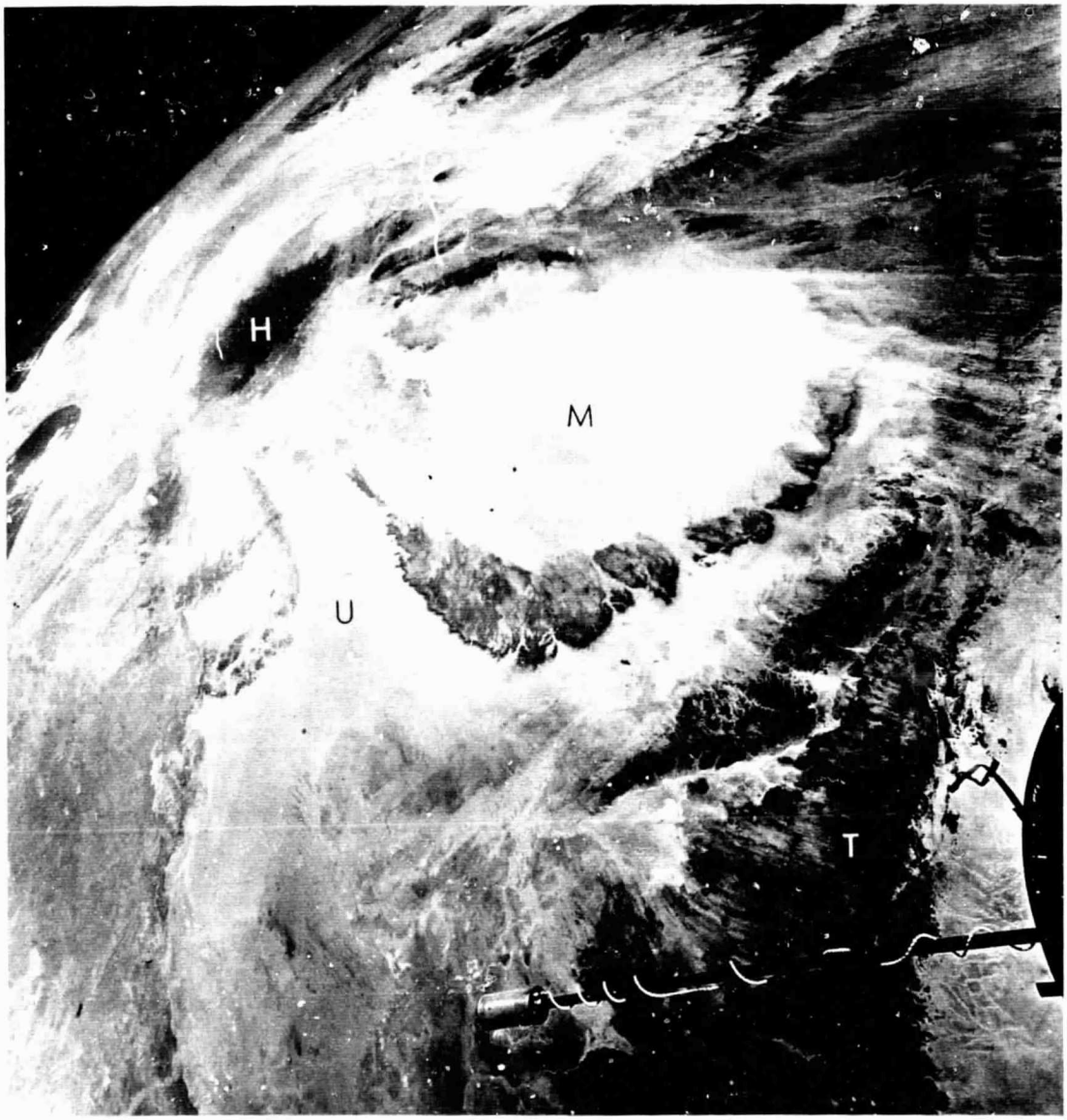

Figure 6. Gemini 11 photo S-66-54526; view to northeast over North Africa, with Mediterranean Sea at upper left. Landmarks as follows: M - Marzuk Sand Sea; H - Haruj al Aswad (Recent volcanic field); U - Ubari Sand Sea; T - Tassili Najjer (Cuesta of Paleozoic sedimentary rock). Marzuk Sand Sea is 320 km wide (NW to SE). Geology of this photo is described in detail by Pesce (1968).

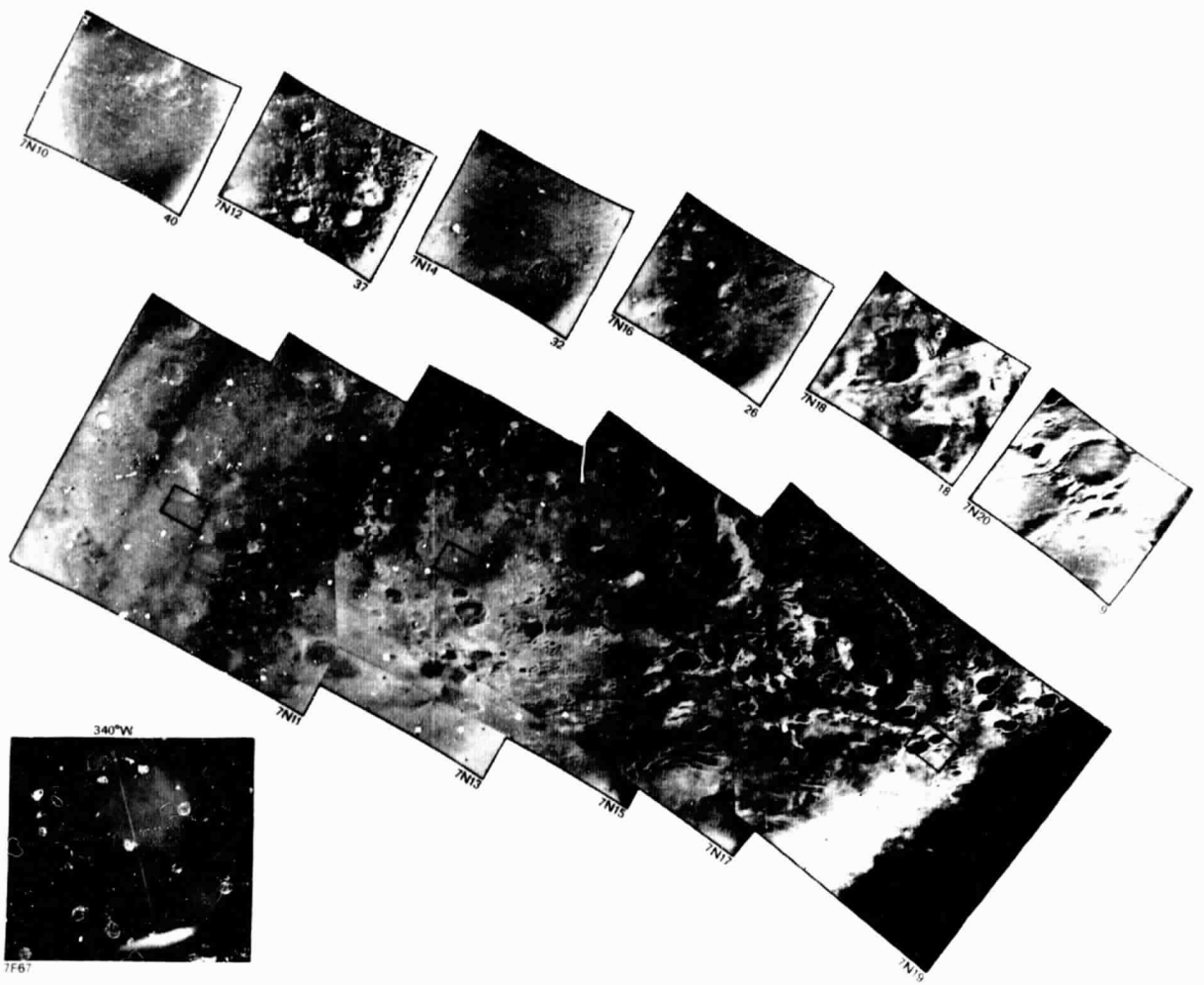

Figure 7. Maximum discriminability mosaic of south polar cap of Mars. Dark band at left is artifact caused by lag in automatic gain control. White band at right is similar artifact in reverse.

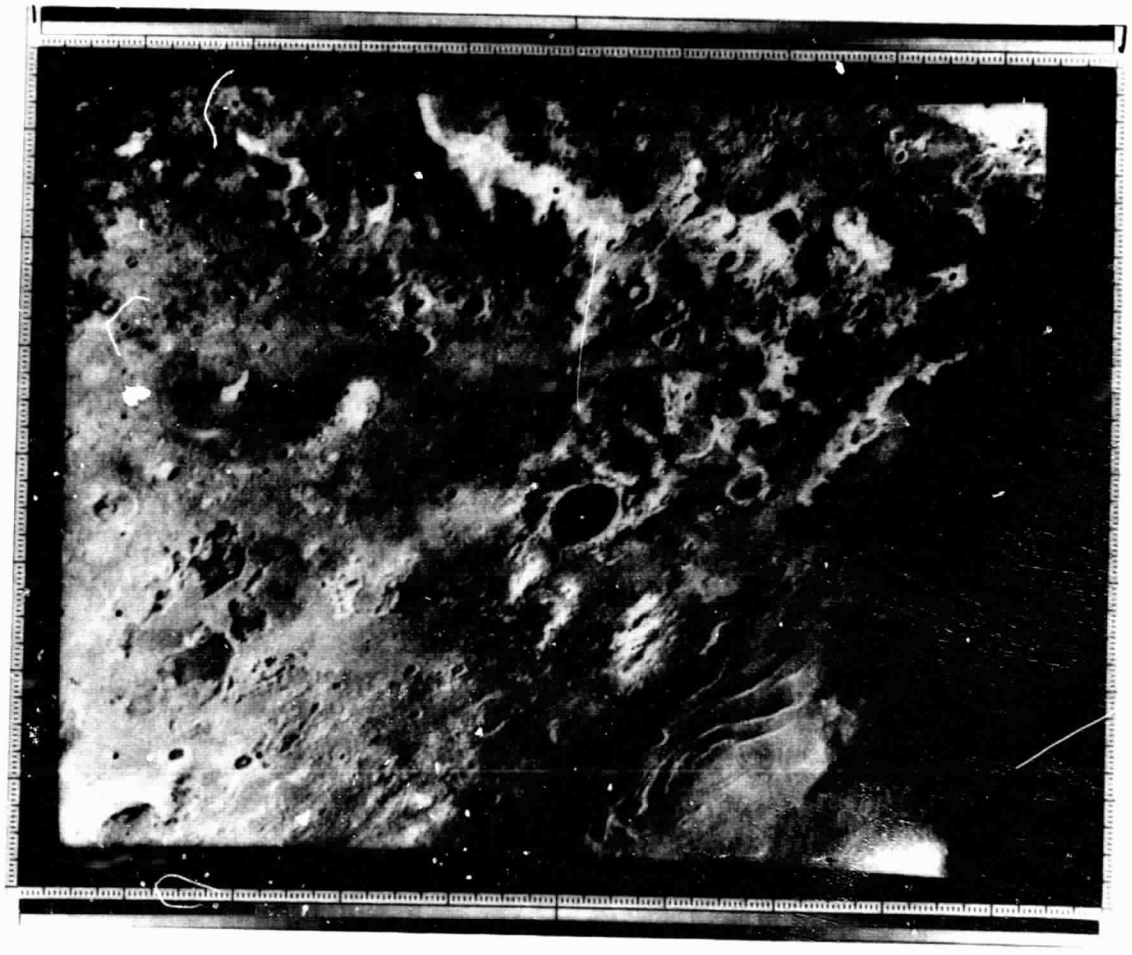

Figure 8. Mariner frame 7N17, A camera, showing ridges near south pole. Area covered 1546 by 1324 km.

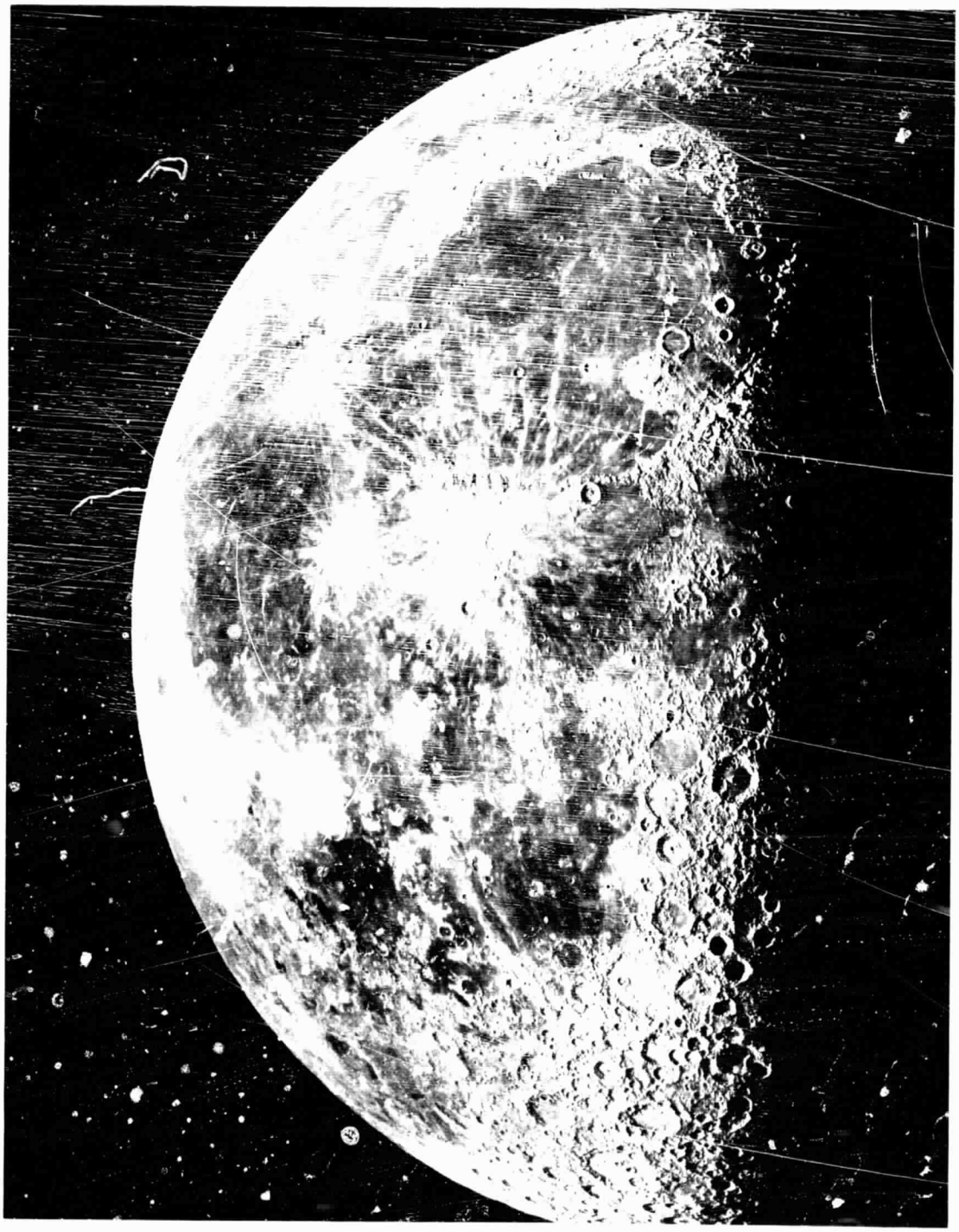

Figure 9. Last-quarter view of the moon with 100 inch Lick reflector, showing Imbrium sculpture (ridges radiating from Mare Imbrium, at top center, to southeast and south). North at top. Photograph courtesy Mount Wilson Observatory.

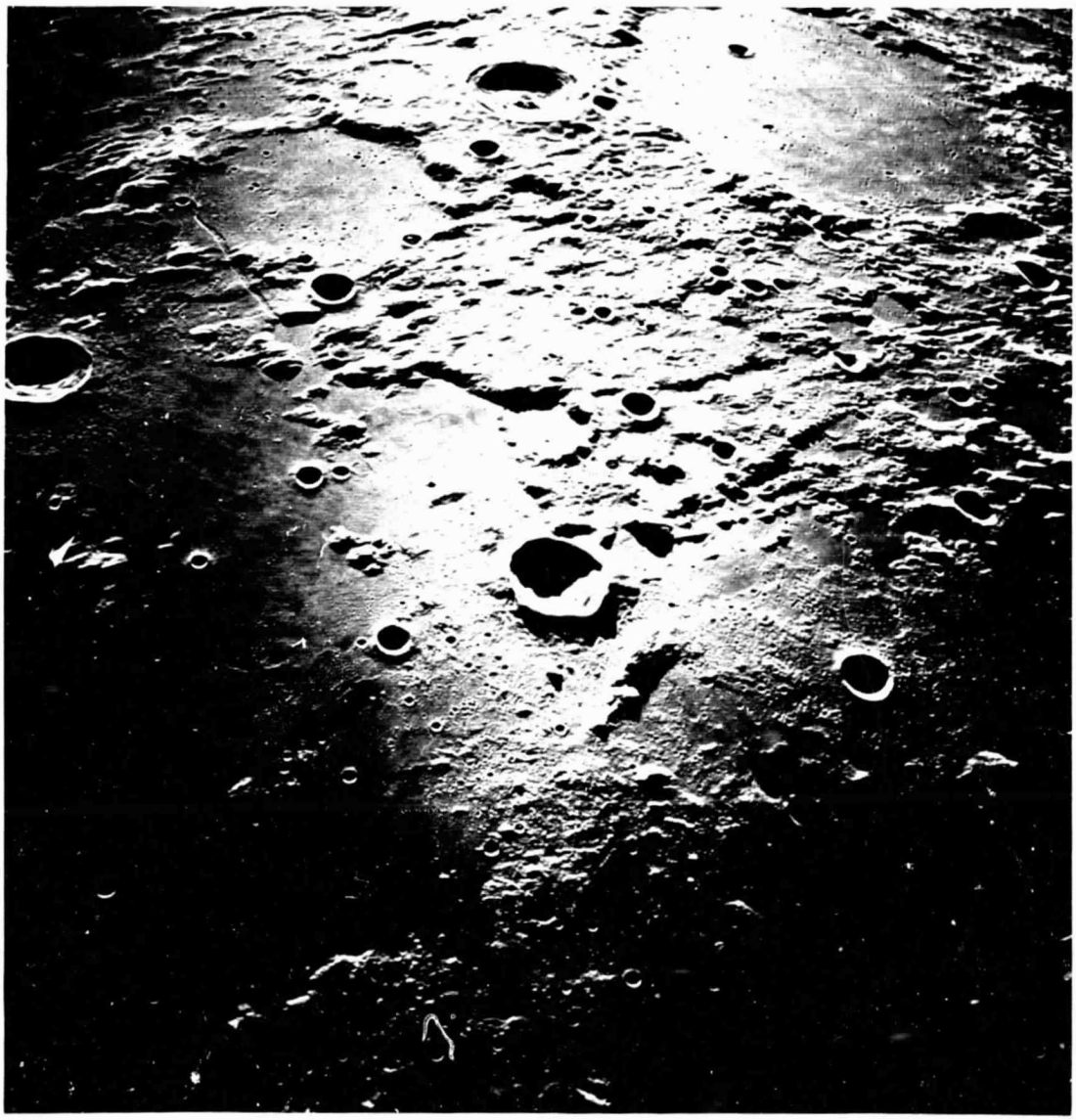

Figure 10. Apollo 12 photo AS 12-50-7435, taken by Astronaut Richard Gordon from about 110 km. View is to southeast, with large crater Ptolemaeus at upper right, showing Imbrium sculpture at closer range. Mare Imbrium would be to the lower left.

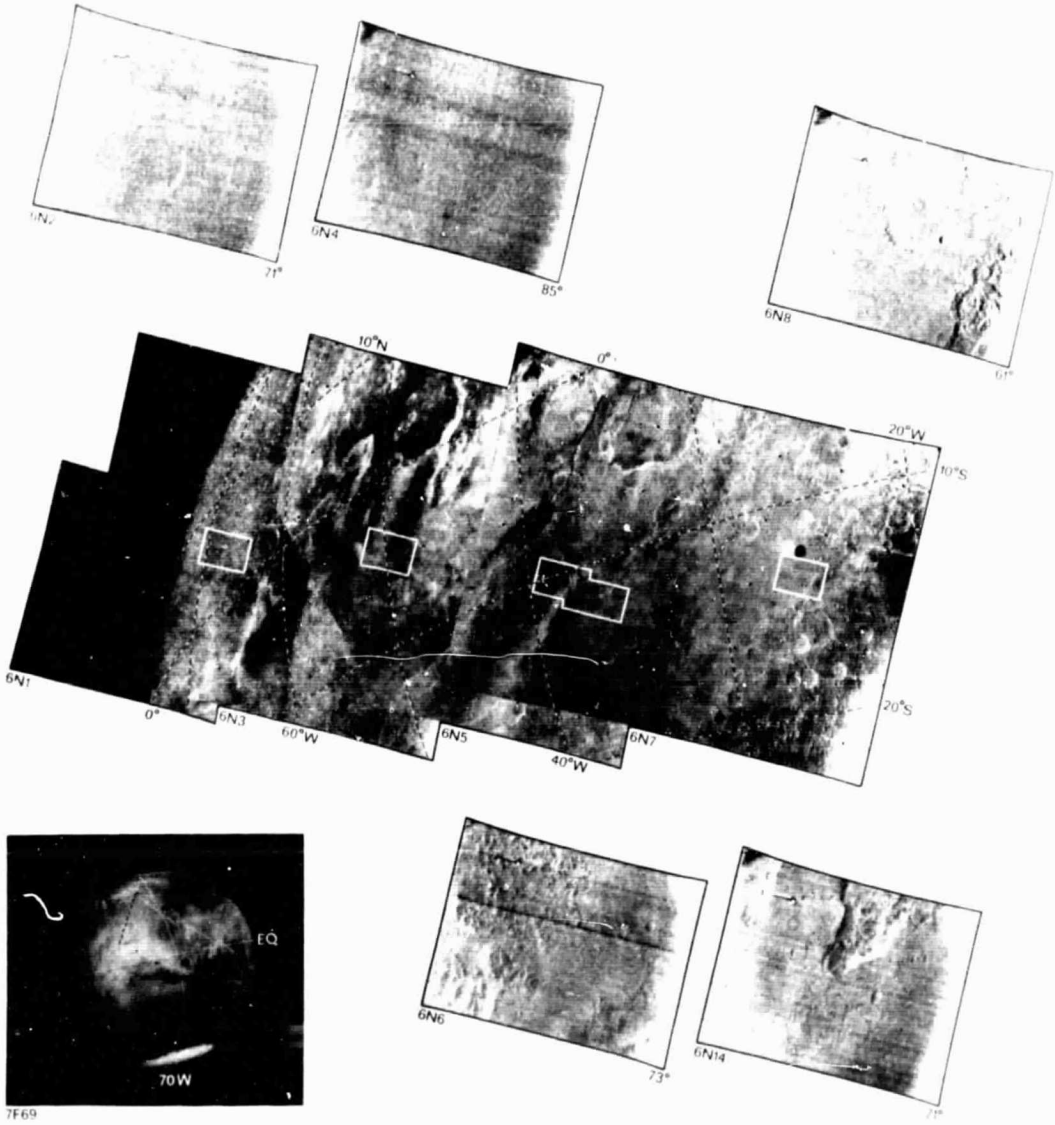

Figure 11. Maximum discriminability mosaic of Mars, showing part of northern hemisphere with chaotic terrain.

Figure 12. Mariner frame 6N7, A camera, covering area 1414 km by 993 km; location of area shown in Figure 11. Cratered terrain at lower right; chaotic terrain at left. Light areas bordering inner slopes of chaotic terrain may be accumulations of sand. Note linear scarps bordering chaotic terrain on east; these appear similar to those bordering the Hellas basin.

Figure 13. Mariner frame 6N14, B camera, covering area 237 by 99 km. Area of cratered terrain at top center is shown at left center of Figure 12.

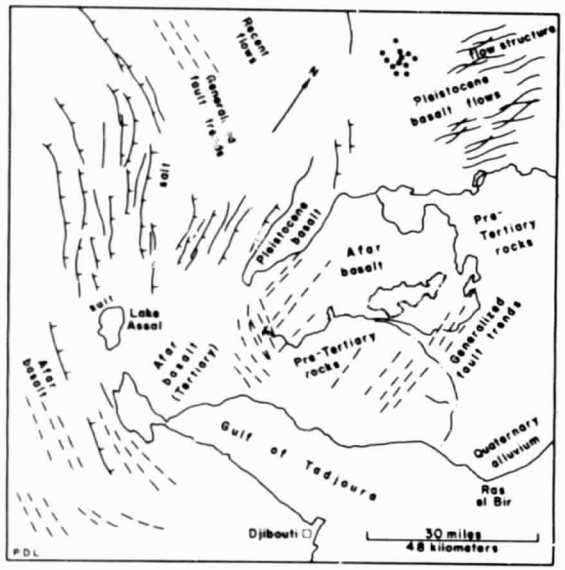

INDEX MAP

APOLLO 9 PHOTOGRAPH AS 9-23-3539

Note: Only main faults shown; hachures on down-dropped block. Contacts not shown completely.

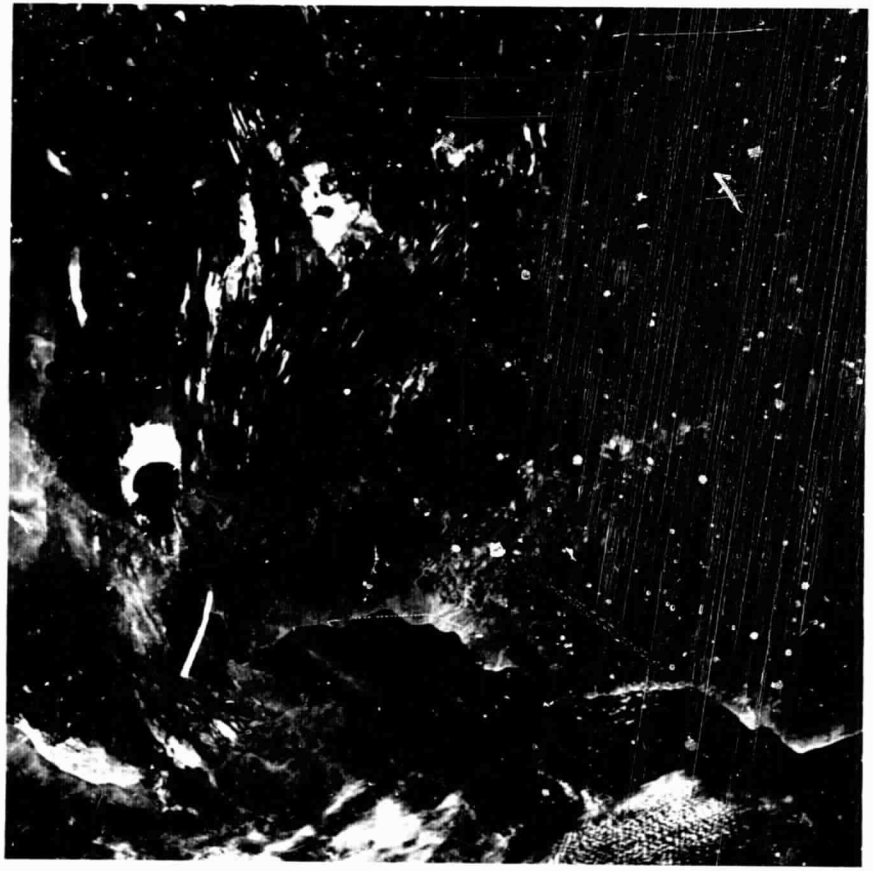

Figure 14. Apollo 9 photo AS 9-23-3539, covering area about 100 km square, in Afar depression; north at top. Linear features are normal fault scarps, produced by extension and breakup of continental crust related to sea floor spreading in Red Sea and Gulf of Aden (Mohr, 1970). Light areas salt deposits; darkest rock lava flows.

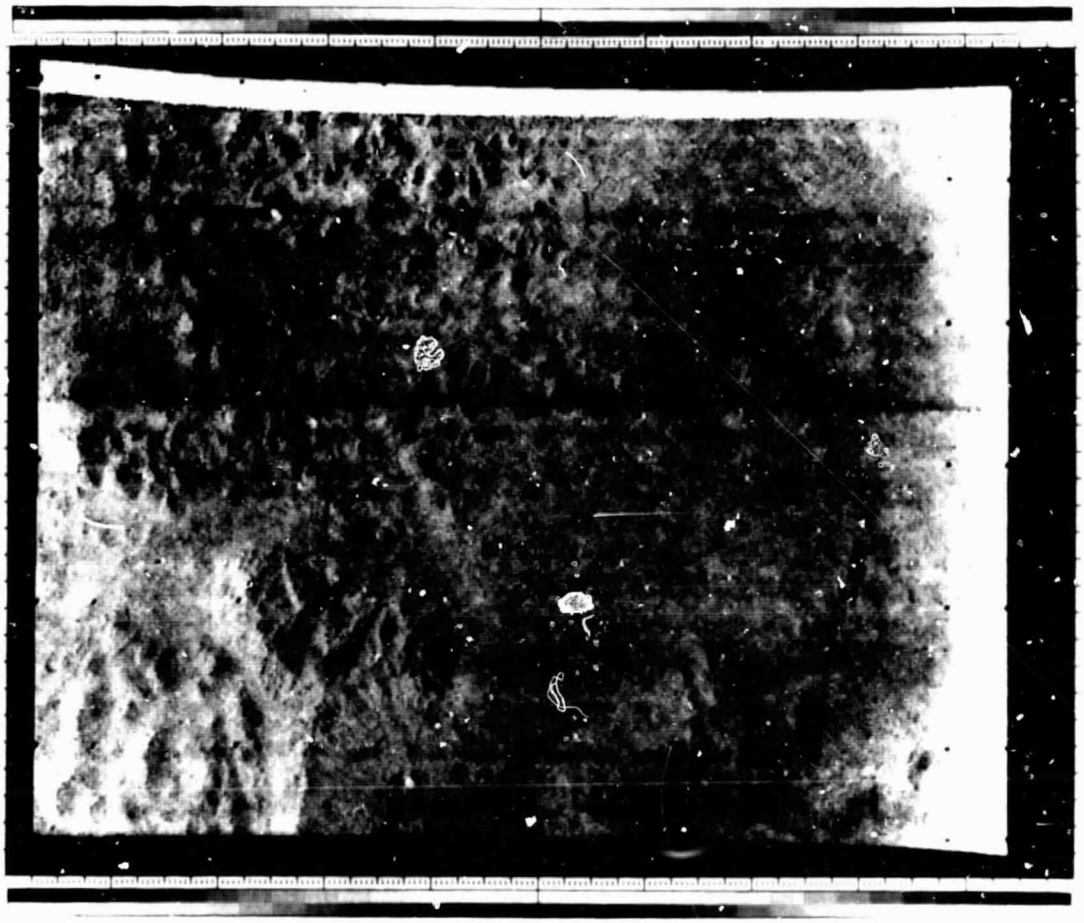

Figure 15. Mariner frame 6N6, B camera, covering area 158 by 108 km; location shown in Figure 11. Chaotic terrain at left.

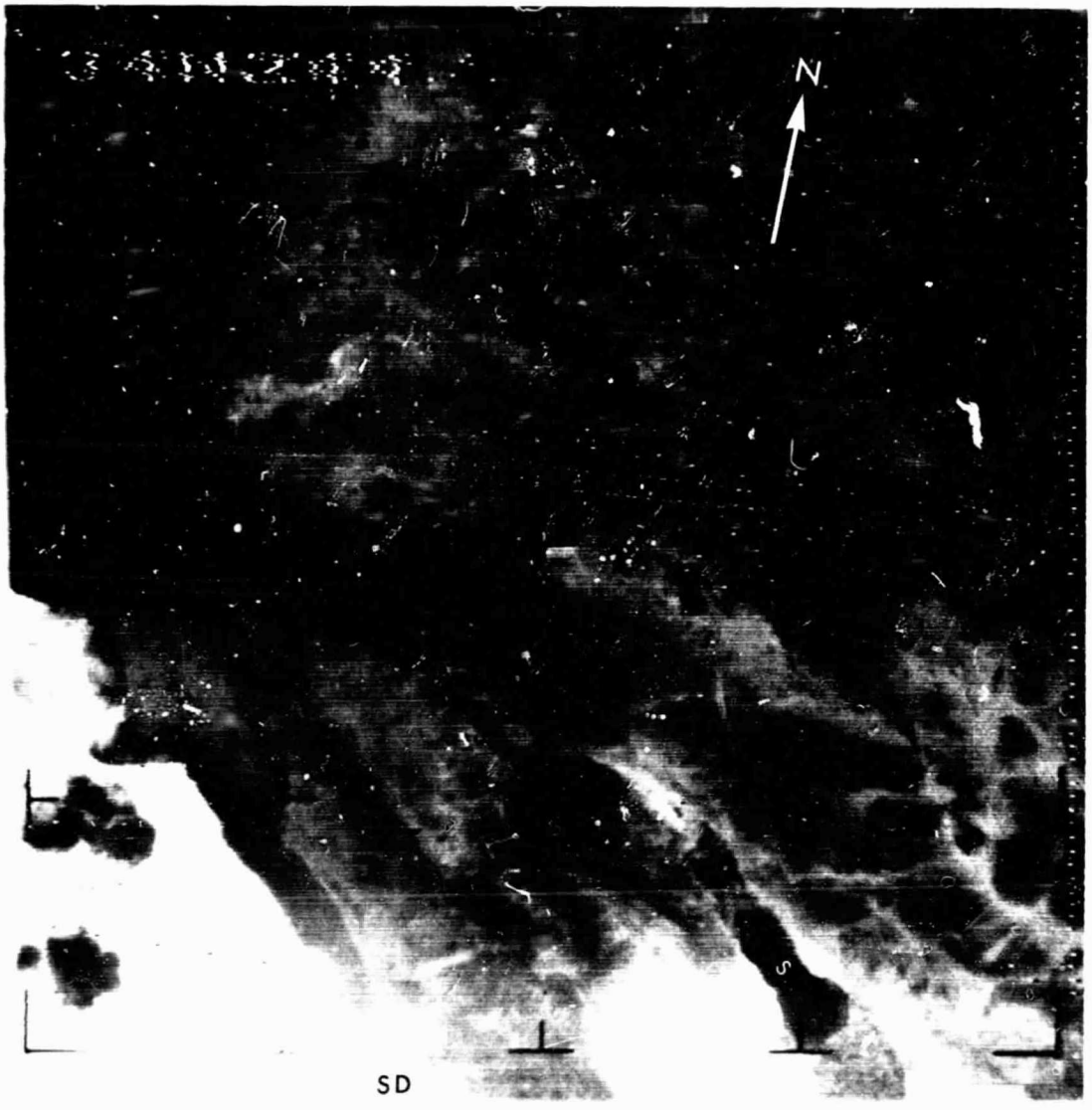

Figure 16. Nimbus I Advanced Vidicon Camera System picture (800 scan lines) of southern California covering area about 320 km square with 1/2 km ground resolution. Dark areas, except for Salton Sea (S) and adjacent farms, are mountains and light areas alluvium-filled valleys. Mojave Desert at upper right. Landmarks as follows: LA - Los Angeles; SB - San Bernadino; SD - Dan Diego; M - Mojave River; 1 - San Andreas fault; 2 - Garlock fault; 3 - San Jacinto fault; 4 - Elsinore fault. Most valleys in Mojave Desert fault controlled.

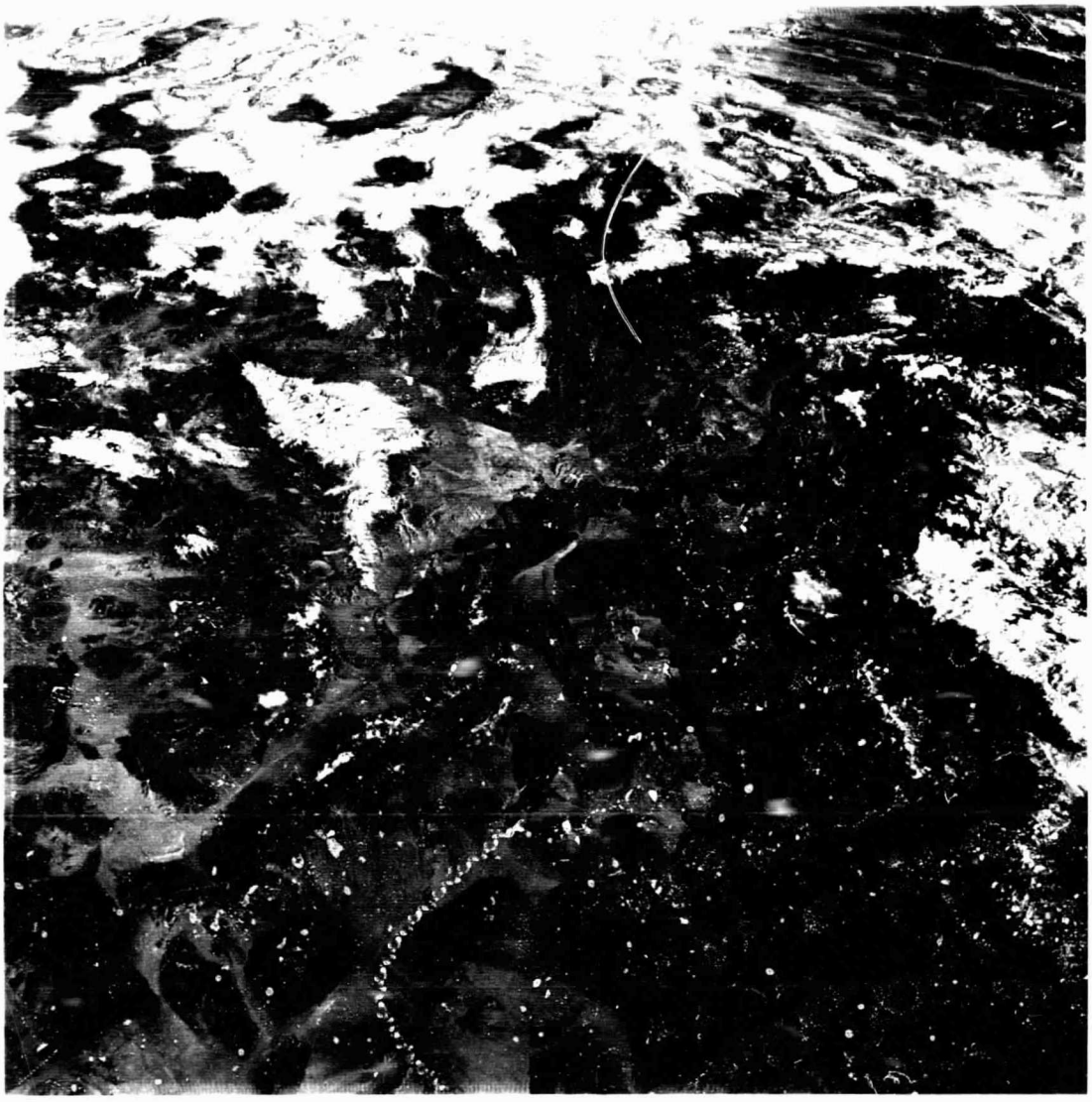

Figure 17. Apollo 9 photo AS 9-20-3135; oblique view to north over eastern part of Mojave Desert; left half of photo overlaps Figure 16. Colorado River at right; Lake Mead and Las Vegas at center. Scale variable; E-W distance at center of photo about 280 km. Area partly snow-covered at north; cirrus clouds at extreme upper right.

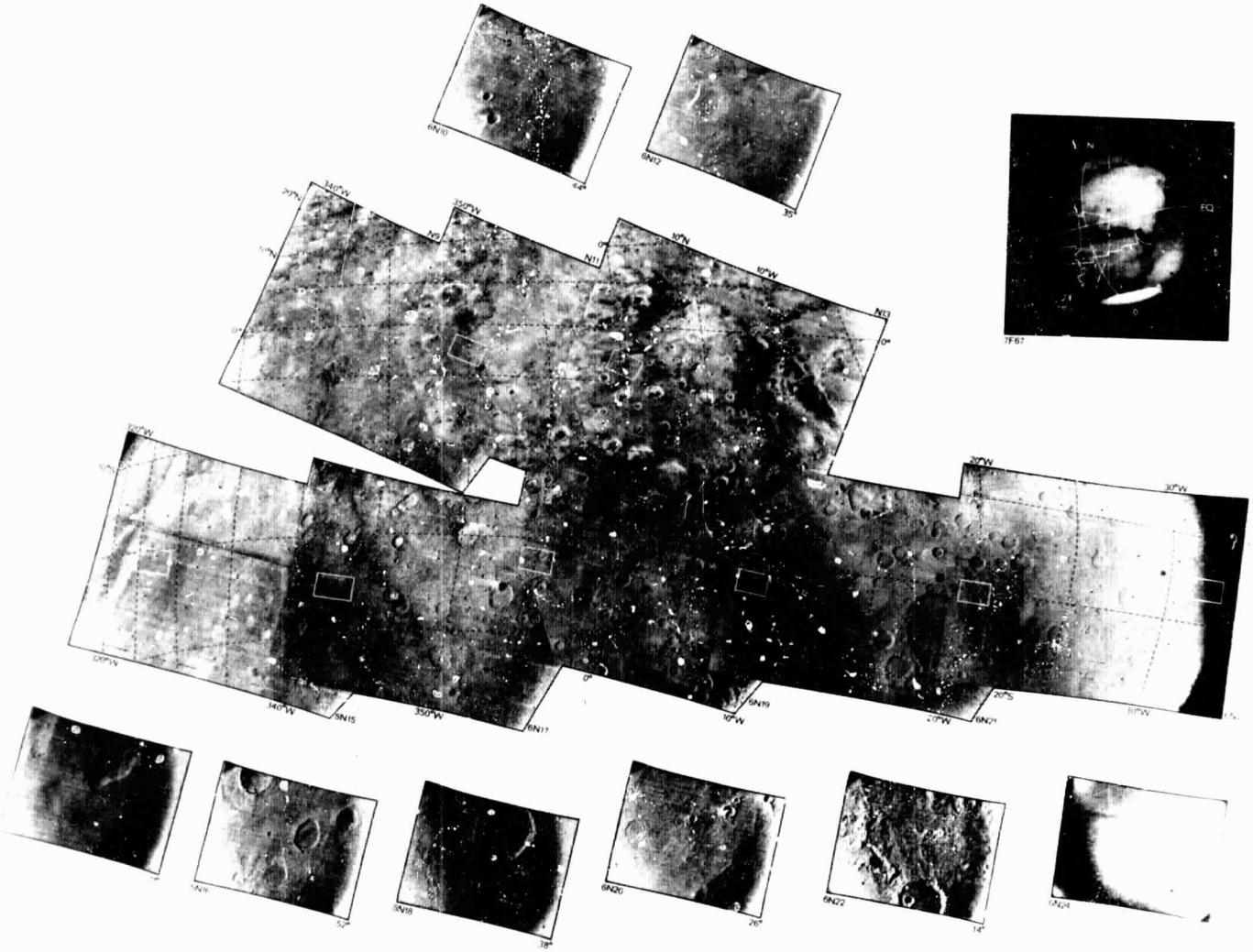

Figure 18. Maximum discriminability mosaic of equatorial region of Mars in vicinity of Deucalionis Regio.

Figure 19. Mariner frame 6N15, A camera, covering area 2507 by 867 km; location shown in Figure 18. Cratered terrain at right. Light-toned linear feature at left interpreted as possible sand deposit area; may be chaotic terrain filled with sand.

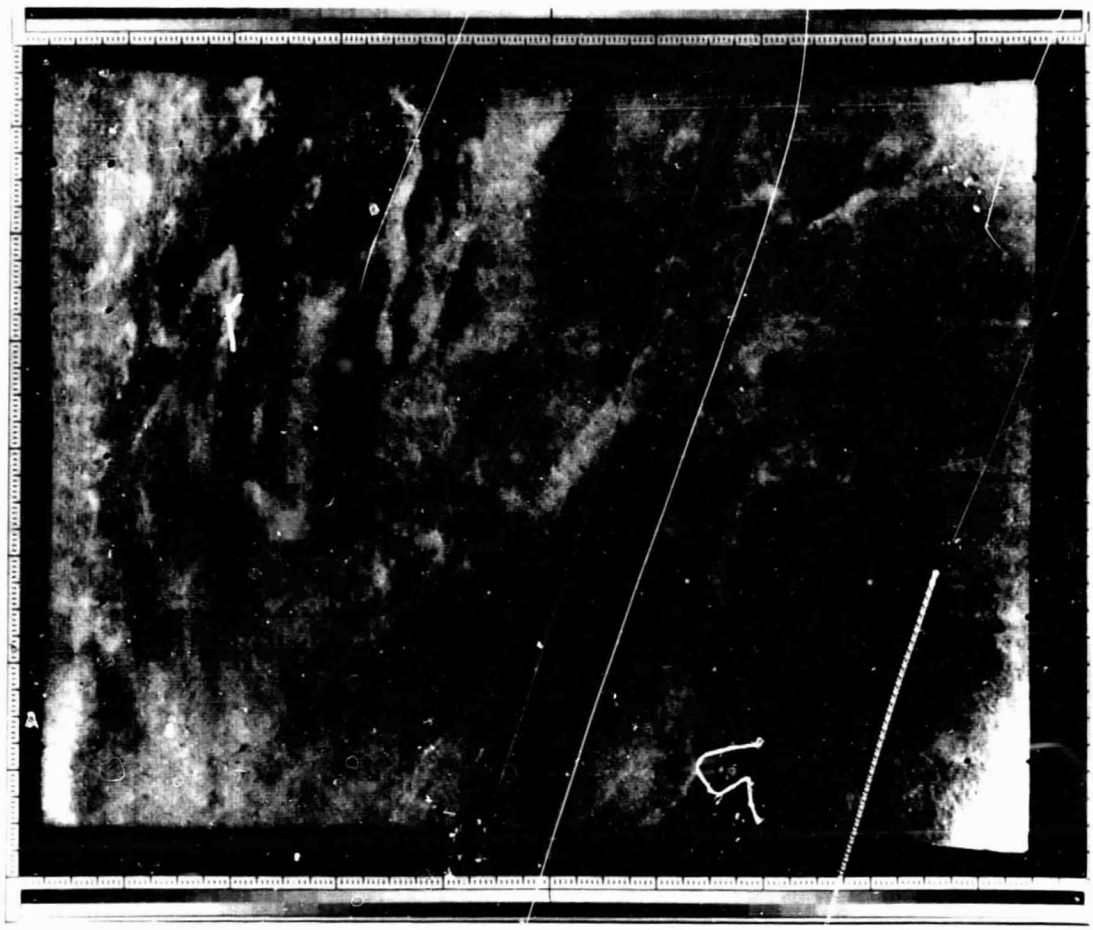

Figure 20. Mariner frame 6N6, A camera, covering area 2277 by 1125 km; location shown in Figure 11; picture overlaps Figure 12. Light-toned sinuous feature at left interpreted as area of sand deposition. Light area near edge of chaotic terrain at center may also be sand deposited near escarpments.

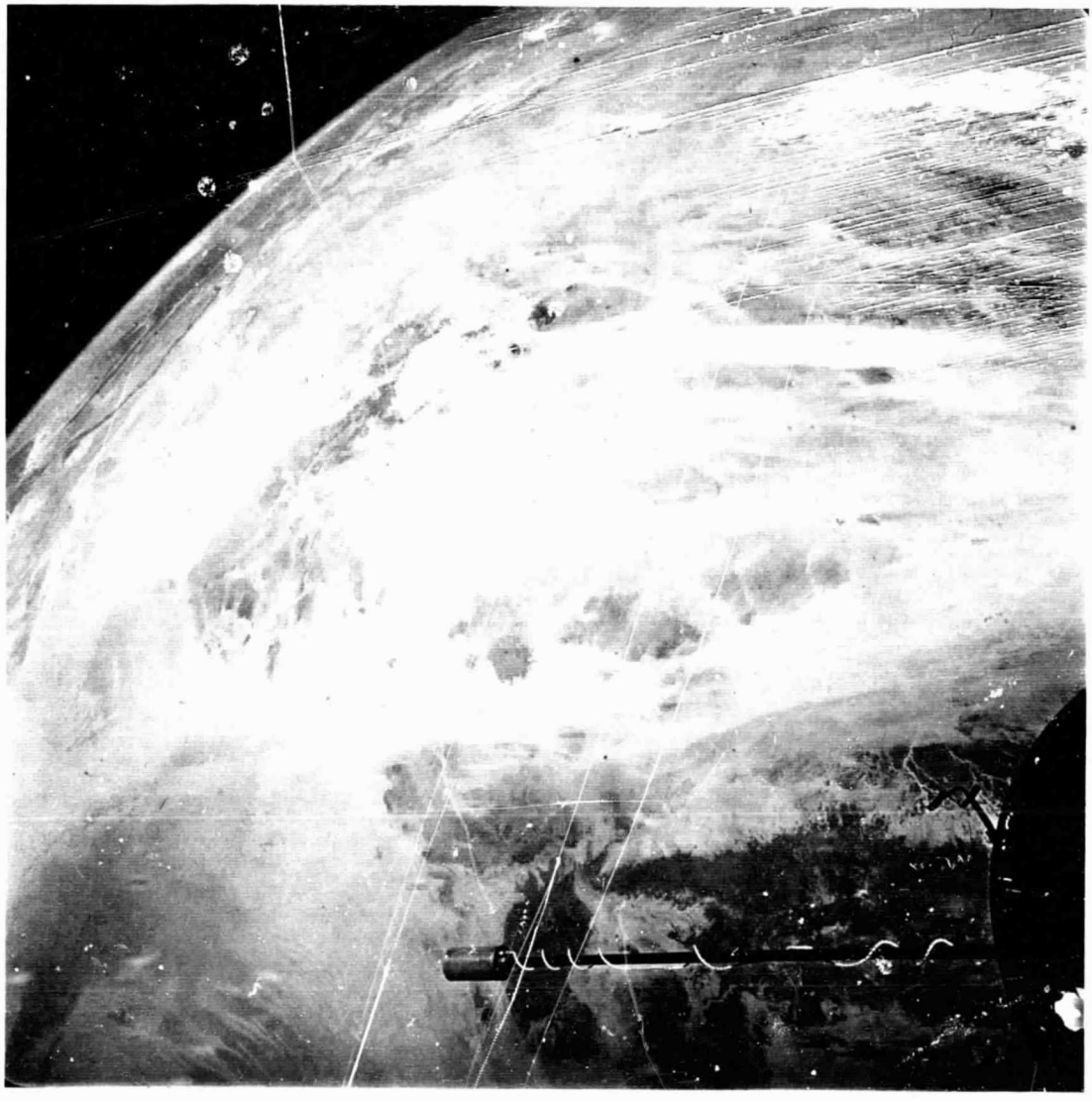

Figure 21. Gemini 11 photo S-66-54528; oblique view to north over northeast Sahara. Light-toned linear features are ergs, typically tens of kilometers in width and hundreds of kilometers in length. See Figure 22 for locations.

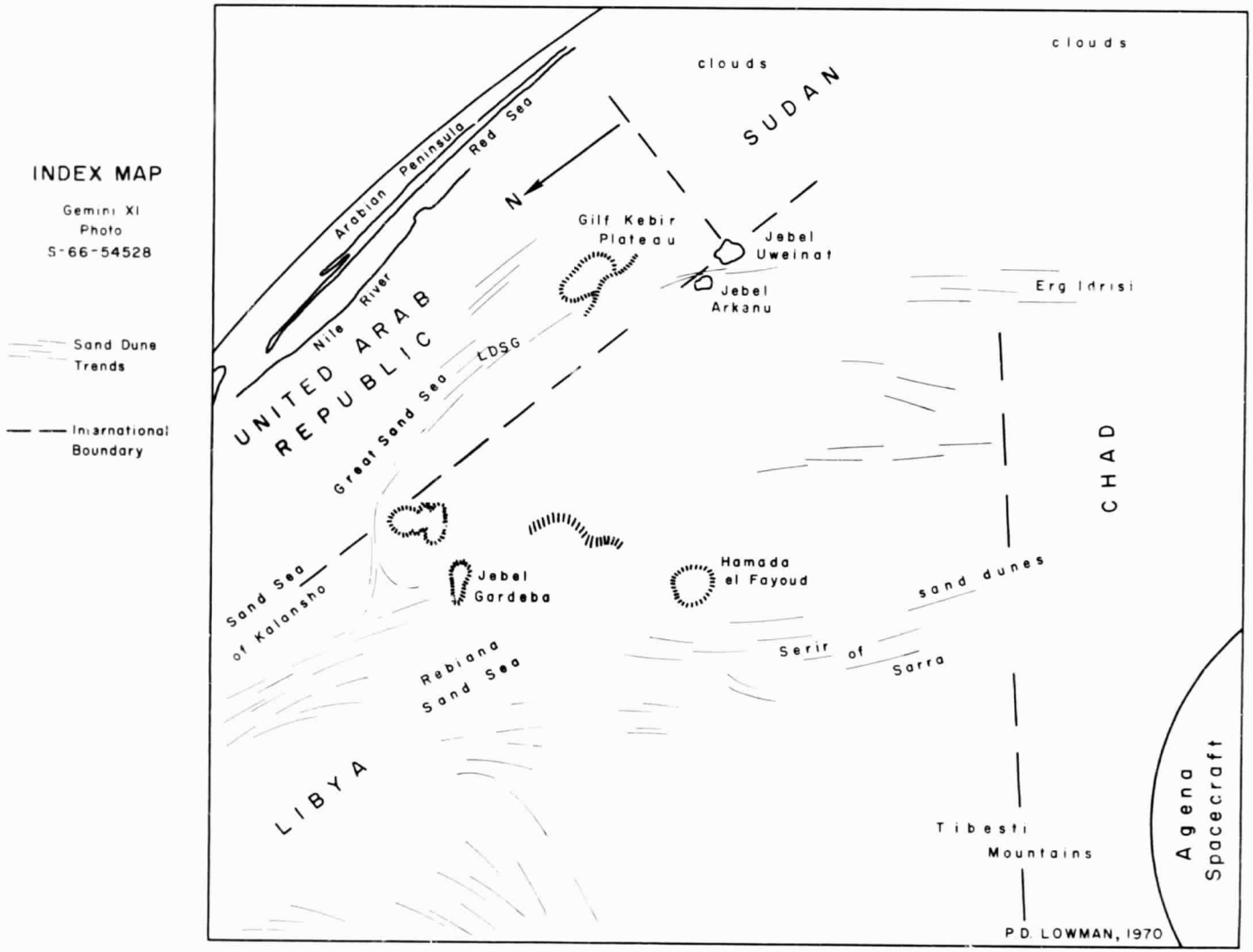

Figure 22. Sketch map of Figure 21.

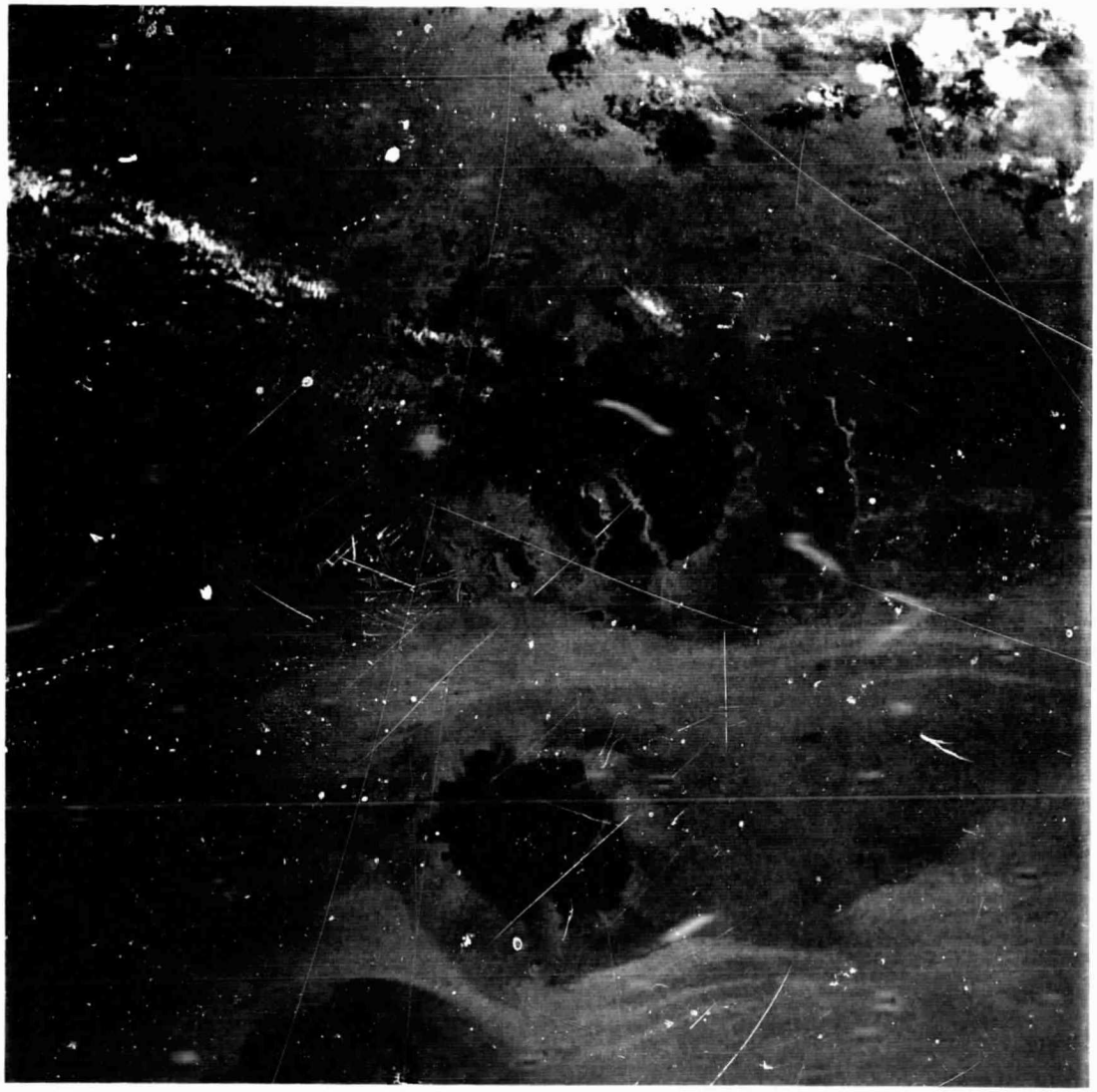

Figure 23. Apollo 9 photo AS 9-23-3533, covering area about 110 km square in northeast Sahara. Mountains in center are Jebel Uweinat and Jebel Arkenu (see Figures 21 and 22 for location), granitic intrusions. Note sharp boundaries of linear ergs.

Figure 24. Mariner frame 6N13, A camera, covering area 1107 by 1139 km in Meridiani Sinus; see Figure 18 for location. Note light-toned material on north floors of craters; this is interpreted as sand deposited in lee of crater walls. Light areas outside craters may also be sand.

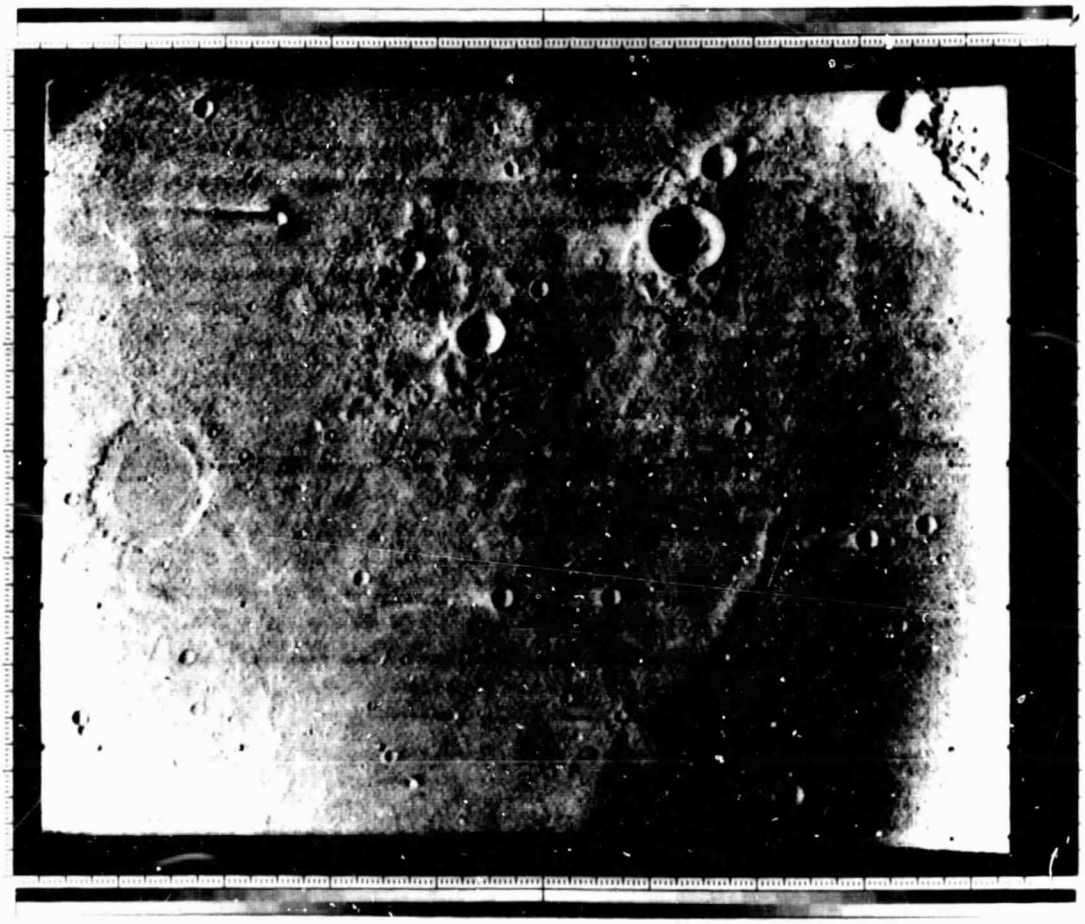

Figure 25. Mariner frame 6N20, B camera, covering area 89 by 73 km south of Meridiani Sinus; see Figure 18 for location. Note ridge at lower right, interpreted as analogous to lunar mare ridges.

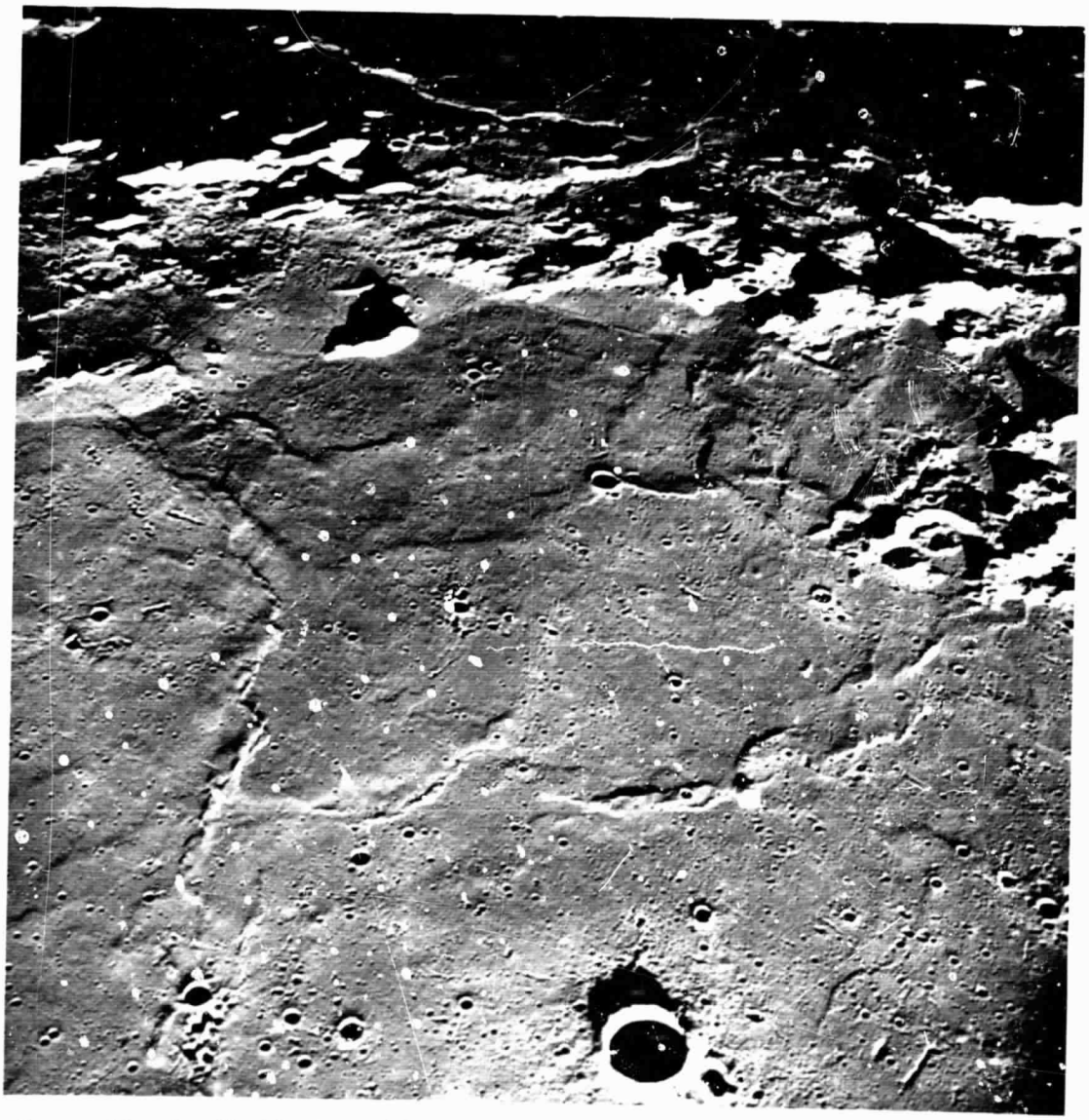

Figure 26. Apollo 10 photo AS 10-27-3907, taken by Apollo 10 crew from lunar orbit, looking west over Sinus Medii, a highland mare near the center of the earthward face. Scale variable; large crater in foreground (Bruce) is about 6 km wide. Compare mare ridges to Figure 25.

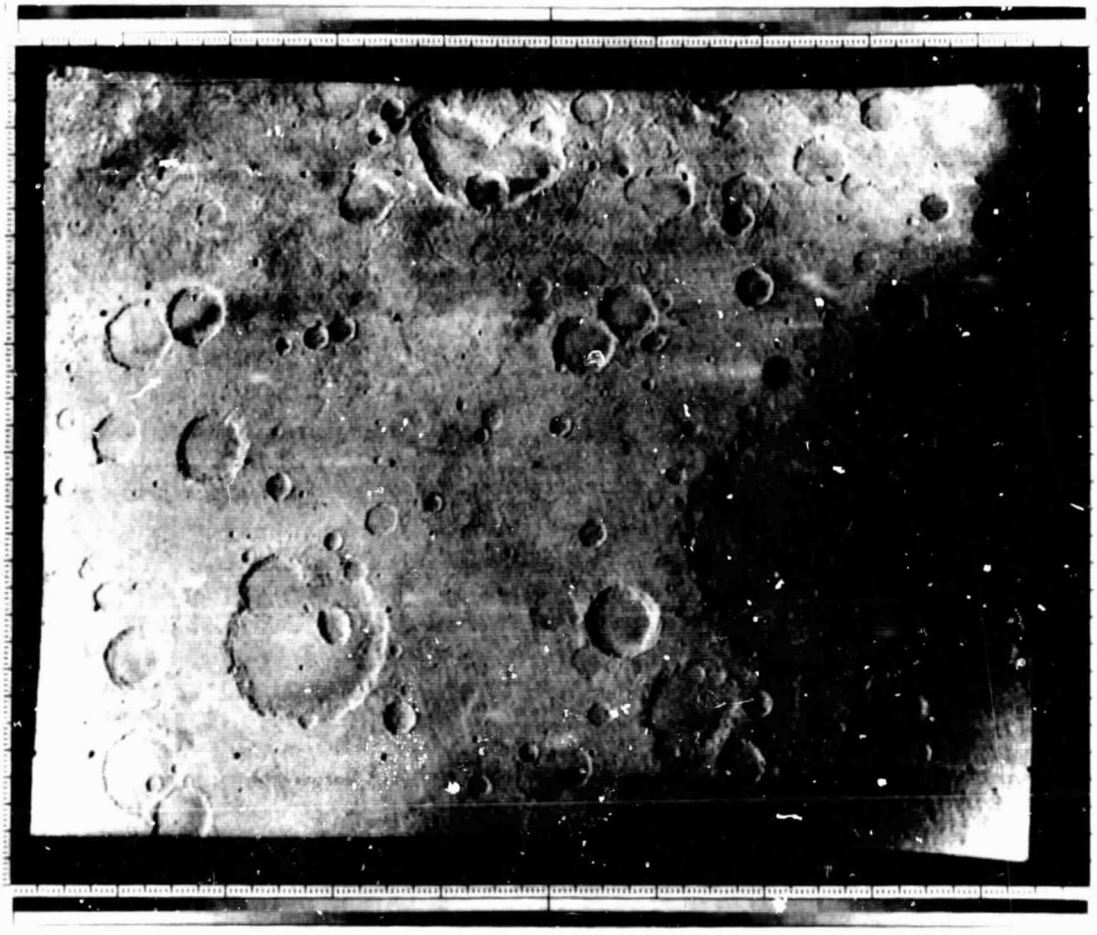

Figure 27. Mariner frame 6N21, A camera, covering area 902 km by 701 km south of Meridiani Sinus; see Figure 18 for location. Sun coming from left; solar zenith angle 70 degrees. Note sinuous rille at top, just south of composite crater.

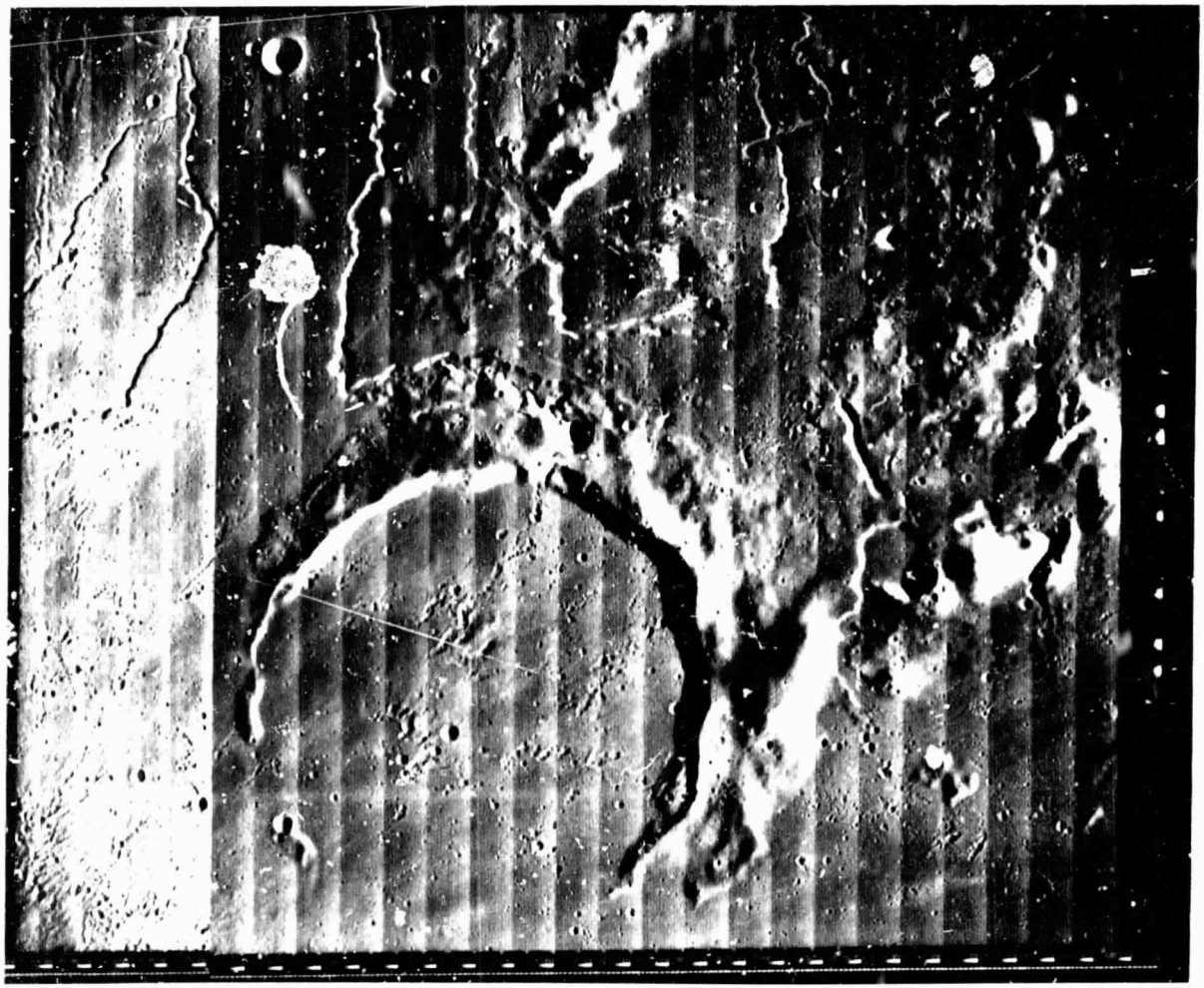

Figure 28. Lunar Orbiter photo V-187M, showing crater Prinz and adjacent rille system. Gradation between sinuous and regular rilles suggests tectonic control for all; see Lowman (1969) for fuller discussion of this photo. Crater Prinz is about 50 km wide.

Figure 29. Portion of USAF Aeronautical Chart and Information Center Map of Mars, MEC-1, (1962) showing prominent landmarks mentioned in text: M - Meridiani Sinus; A - Aurorae Sinus; S - Syrtis Major; H - Hellas; Hp - Hellespontus. Note: Map is based on pre-Mariner 4 telescopic observations; most canals shown do not exist. See Cutts, et al., (1971), for discussion of this point.

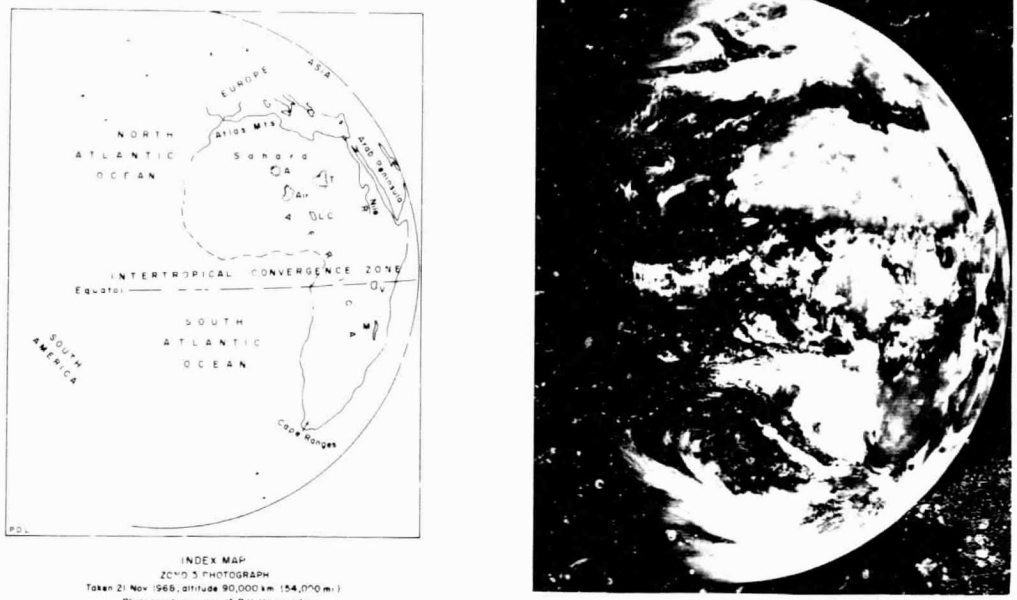

Figure 30. Zond 5 photographs of Africa from 90,000 kilometers, with index maps. Note general similarity between darks massif pattern of Africa and Mars. The Zond 5 photographs were provided by Dr. B. V. Vinogradov.

FIGURE CAPTIONS

Figure 1. Mariner frame 7F67, B camera (508 mm focal length), from 710,814 km range, showing Mars with north at top. Hellas indicated by arrow.

Figure 2. Mariner frame 6F49, B camera, from 206,681 km range, showing Hellas at lower right.

Figure 3. Mariner frame 7N25, A camera (52.5 mm focal length), showing cratered terrain of Hellespontus. North at top; area covered 1228 by 723 km. Slope down into Hellas basin at upper right. This and all other photos are "maximum discriminability" versions unless otherwise labeled.

Figure 4. Mariner frame 7N27, A camera, showing slope from Hellespontus into Hellas. Area covered 998 by 723 km; overlaps previous picture. Black dots are reseau marks; white streaks to their left are artifacts caused by slow decay of automatic gain control (Dunne, et al., 1971).

Figure 5. Apollo 6 photo AS 6-2-1450, covering area averaging 150 km square in southern New Mexico and west Texas; north at bottom. Landmarks as follow: cb - Carlsbad, N.M.; P - Pecos River; C - Guadalupe Ridge (exhumed Paleozoic reef); H - Huapache monocline; B - Broke-off Mountains; GM - Guadalupe Mountains; D - Delaware Mountains; S - Salt Basin (squares are cultivated land); Y - Y-O Structural Zone (Dane and Bachman, 1964); SM - Sacramento Mountains. Scratch-like mark above "B" is scratch. Most of area underlain by late Paleozoic carbonates. West face of Guadalupe Mountains

fault scarp, with east side (left) upthrown. Brokeoff Mountains are fault slices; compare with scarps in Figures 3 and 4 between Hellas and Hellespontus.

Figure 6. Gemini 11 photo S-66-54526; view to northeast over North Africa, with Mediterranean Sea at upper left. Landmarks as follow: M - Marzuk Sand Sea; H - Haruj al Aswad (Recent volcanic field); U - Ubari Sand Sea; T - Tassili Najjer (cuesta of Paleozoic sedimentry rock). Marzuk Sand Sea is 320 km wide (NW to SE). Geology of this photo is described in detail by Pesce (1968).

Figure 7. Maximum discriminability mosaic of south polar cap of Mars. Dark band at left is artifact caused by lag in automatic gain control. White band at right is similar artifact in reverse.

Figure 8. Mariner frame 7N17, A camera, showing ridges near south pole. Area covered 1546 by 1324 km.

Figure 9. Last-quarter view of the moon with 100 inch Lick reflector, showing Imbrium sculpture (ridges radiating from Mare Imbrium, at top center, to southeast and south). North at top. Photograph courtesy Mount Wilson Observatory.

Figure 10. Apollo 12 photo AS 12-50-7435, taken by Astronaut Richard Gordon from about 110 km. View is to southeast, with large crater Ptolemaeus at upper right, showing Imbrium sculpture at closer range. Mare Imbrium would be to the lower left.

Figure 11. Maximum discriminability mosaic of Mars, showing part of northern hemisphere with chaotic terrain.

Figure 12. Mariner frame 6N7, A camera, covering area 1414 km by 993 km; location of area shown in Figure 11. Cratered terrain at lower right; chaotic terrain at left. Light areas bordering inner slopes of chaotic terrain may be accumulations of sand. Note linear scraps bordering chaotic terrain on east; these appear similar to those bordering the Hellas basin.

Figure 13. Mariner frame 6N14, B camera, covering area 237 by 99 km. Area of cratered terrain at top center is shown at left center of Figure 12.

Figure 14. Apollo 9 photo AS 9-23-3539, covering area about 100 km square, in Afar depression; north at top. Linear features are normal fault scarps, produced by extension and breakup of continental crust related to sea floor spreading in Red Sea and Guld of Aden (Mohr, 1970). Light areas salt deposits; darkest rock lava flows.

Figure 15. Mariner frame 6N6, B camera, covering area 158 by 108 km; location shown in Figure 11. Chaotic terrain at left.

Figure 16. Nimbus I Advanced Vidicon Camera System picture (800 scan lines) of southern California covering area about 320 km square with 1/2 km ground resolution. Dark areas, except for Salton Sea (S) and adjacent farms, are mountains and light areas alluvium-filled valleys. Mojave Desert at upper right. Landmarks as follows: LA - Los

Angeles; SB - San Bernadino; SD - San Diego; M - Mojave River; 1 - San Andreas fault; 2 - Garlock fault; 3 - San Jacinto fault; 4 - Elsinore fault. Most valleys in Mojave Desert fault controlled.

Figure 17. Apollo 9 photo AS 9-20-3135; oblique view to north over eastern part of Mojave Desert; left half of photo overlaps Figure 16. Colorado River at right; Lake Mead and Las Vegas at center. Scale variable; E-W distance at center of photo about 280 km. Area partly snow-covered at north; cirrus clouds at extreme upper right.

Figure 18. Maximum discriminability mosaic of equatorial region of Mars in vicinity of Deucalionis Regio.

Figure 19. Mariner frame 6N15, A camera, covering area 2507 by 867 km; location shown in Figure 18. Cratered terrain at right. Light-toned linear feature at left interpreted as possible sand deposit area; may be chaotic terrain filled with sand.

Figure 20. Mariner frame 6N5, A camera, covering area 2277 km by 1125 km, location shown in Figure 11; picture overlaps Figure 12. Light-toned sinuous feature at left interpreted as area of sand deposition. Light areas near edge of chaotic terrain at center may also be sand deposited near escarpments.

Figure 21. Gemini 11 photo S-66-54528; oblique view to north over northeast Sahara. Light-toned linear features are ergs, typically tens of kilometers in width and hundreds of kilometers in length. See Figure 22 for locations.

Figure 22. Sketch map of Figure 21.

Figure 23. Apollo 9 photo AS 9-23-3533, covering area about 110 km square in northeast Sahara. Mountains in center are Jebel Uweinat and Jebel Arkenu (see Figs. 21 and 22 for location), granitic intrusions. Note sharp boundaries of linear ergs.

Figure 24. Mariner frame 6N13, A camera, covering area 1107 by 1139 km in Meridiani Sinus; see Figure 18 for location. Note light-toned material on north floors of craters; this is interpreted as sand deposited in lee of crater walls. Light areas outside craters may also be sand.

Figure 25. Mariner frame 6N20, B camera, covering area 89 by 73 km south of Meridiani Sinus; see Figure 18 for location. Note ridge at lower right, interpreted as analogous to lunar mare ridges.

Figure 26. Apollo 10 photo AS 10-27-3907, taken by Apollo 10 crew from lunar orbit, looking west over Sinus Medii, a highland mare near the center of the earthward face. Scale variable; large crater in foreground (Bruce) is about 6 km wide. Compare mare ridges to Figure 25.

Figure 27. Mariner frame 6N21, A camera, covering area 902 km by 701 km south of Meridiani Sinus; see Figure 18 for location. Sun coming from left; solar zenith angle 70 degrees. Note rille at top, just south of composite crater.

Figure 28. Lunar Orbiter photo V-187M, showing crater Prinz and adjacent rille system. Gradation between sinuous and regular rilles suggests tectonic control for all; see Lowman (1969) for fuller discussion of this photo. Crater Prinz is about 50 km wide.

Figure 29. Portion of USAF Aeronautical Chart and Information Center Map of Mars, MEC-1, (1962) showing prominent landmarks mentioned in text: M - Meridiani Sinus; A - Aurorae Sinus; S - Syrtis Major; H - Hellas; Hp - Hellespontus. Note: Map is based on pre-Mariner 4 telescopic observations; most canals shown do not exist. See Cutts, et al., (1971) for discussion of this point.

Figure 30. Zond 5 photographs of Africa from 90,000 kilometers, with index maps. Note general similarity between darks massif pattern of Africa and Mars. The Zond 5 photographs were provided by Dr. B. V. Vinogradov.